ANNUAL REVIEWS

Tectonic Evolution of the Central Andean Plateau and Implications for the Growth of Plateaus*

Carmala N. Garzione,[1] Nadine McQuarrie,[2]
Nicholas D. Perez,[3,4] Todd A. Ehlers,[5] Susan L. Beck,[6]
Nandini Kar,[1,7] Nathan Eichelberger,[8]
Alan D. Chapman,[9] Kevin M. Ward,[6]
Mihai N. Ducea,[6,10] Richard O. Lease,[11]
Christopher J. Poulsen,[12] Lara S. Wagner,[13]
Joel E. Saylor,[14] George Zandt,[6] and Brian K. Horton[3]

ANNUAL REVIEWS **Further**

Click here to view this article's online features:
• Download figures as PPT slides
• Navigate linked references
• Download citations
• Explore related articles
• Search keywords

Keywords

Abstract

Current end-member models for the geodynamic evolution of orogenic plateaus predict (*a*) slow and steady rise during crustal shortening and ablative subduction (i.e., continuous removal) of the lower lithosphere or (*b*) rapid surface uplift following shortening, which is associated with punctuated removal of dense lower lithosphere and/or lower crustal flow. This review integrates results from recent studies of the modern lithospheric structure, geologic evolution, and surface uplift history of the Central Andean Plateau to evaluate the geodynamic processes involved in forming it. Comparison of the timing, magnitude, and distribution of shortening and surface uplift, in combination with other geologic evidence, highlights the pulsed nature of plateau growth. We discuss specific regions and time periods that show evidence for end-member geodynamic processes, including middle–late Miocene surface uplift of the southern Eastern Cordillera and Altiplano associated with shortening and ablative subduction, latest Oligocene–early Miocene and late Miocene–early Pliocene punctuated removal of dense lower lithosphere in the Eastern Cordillera and Altiplano, and late Miocene–early Pliocene crustal flow in the central and northern Altiplano.

1. INTRODUCTION

The mechanisms that build broad, high-elevation orogenic plateaus remain debated because many regions lack the full complement of geologic evidence necessary to document the driving processes. The Central Andean Plateau is the largest orogenic plateau on Earth formed in an oceanic-continental subduction setting. As an active mountain belt, it provides an excellent natural laboratory to study a variety of plateau-building processes.

This review focuses on the ∼50-Ma-to-present development of the Central Andean Plateau, here defined as the high-elevation (>3 km) region encompassing the Altiplano basin, the Western Cordillera, and the Eastern Cordillera between ∼13°S and 22°S (**Figure 1**). At ∼4–6 km elevations, the Western Cordillera magmatic arc and the Eastern Cordillera fold-thrust belt frame the internally drained Altiplano basin (∼4 km elevation). Of particular interest are the timing and geodynamic mechanisms of plateau uplift and the processes by which the continental crust overriding plate has been shortened and thickened, whereas the mantle lithosphere that originally underlay it has been thinned or entirely removed.

Two end-member processes have been proposed for removal of dense lower lithosphere beneath the Central Andean Plateau: (*a*) ablative subduction of mantle lithosphere on the foreland (eastern) side of the system (e.g., Tao & O'Connell 1992, Pope & Willett 1998; see also **Figure 2a**) and (*b*) rapid removal of a thick portion of the lower lithosphere (e.g., Bird 1978, Houseman et al. 1981, Sobolev & Babeyko 2005, Krystopowicz & Currie 2013; **Figure 2b**). These end-member mechanisms are associated with different rates and timing of plateau uplift. Ablative (continuous) subduction of lower lithosphere would correspond with protracted crustal thickening and gradual plateau uplift over tens of millions of years; rapid removal of lower crust and mantle lithosphere would occur after significant crustal thickening and the formation of a high-density eclogitic crustal root (Sobolev & Babeyko 2005, Krystopowicz & Currie 2013), resulting in rapid surface uplift, by 1 km or more over a shorter period of time (e.g., several Myr).

Both end-member processes for lithospheric removal may depend on a wide variety of other phenomena that contribute to the geologic development and surface uplift history of the Central Andean Plateau. These include thermal weakening of the mantle lithosphere due to hydration of the mantle wedge during flat slab subduction (Isacks 1988, James & Sacks 1999), flow of middle or lower crust from regions of high elevation and thick crust to regions of lower elevation and thinner crust (e.g., Husson & Sempere 2003; **Figure 2c**), or magmatic addition of low-density crust (e.g., Perkins et al. 2016; **Figure 2d**).

In this review, we present geologic and paleoelevation constraints on the timing and geodynamic mechanisms of plateau surface uplift and the processes by which lower lithosphere is removed. Geologic evidence includes modern lithospheric structure determined from broadband seismology; geochemical data that constrain the timing and sources of magmatism; Altiplano basin evolution; and the age, magnitude, and distribution of crustal shortening. On the basis of proxy data, we also present constraints on the surface uplift of the Central Andean Plateau for the past 30 Myr. We integrate these results to explore the geodynamic mechanisms of plateau growth, with emphasis on links between the timing and spatial distribution of episodes of shortening, crustal thickening, and plateau surface uplift.

2. SEISMOLOGIC CONSTRAINTS ON LITHOSPHERIC STRUCTURE

The lithospheric structure of the Central Andean Plateau has long been of interest; however, a lack of seismic station coverage, especially in the central and northern Plateau regions, has hampered its imaging. Previous studies in the central Plateau (16°–21°S) identified thick crust with slow
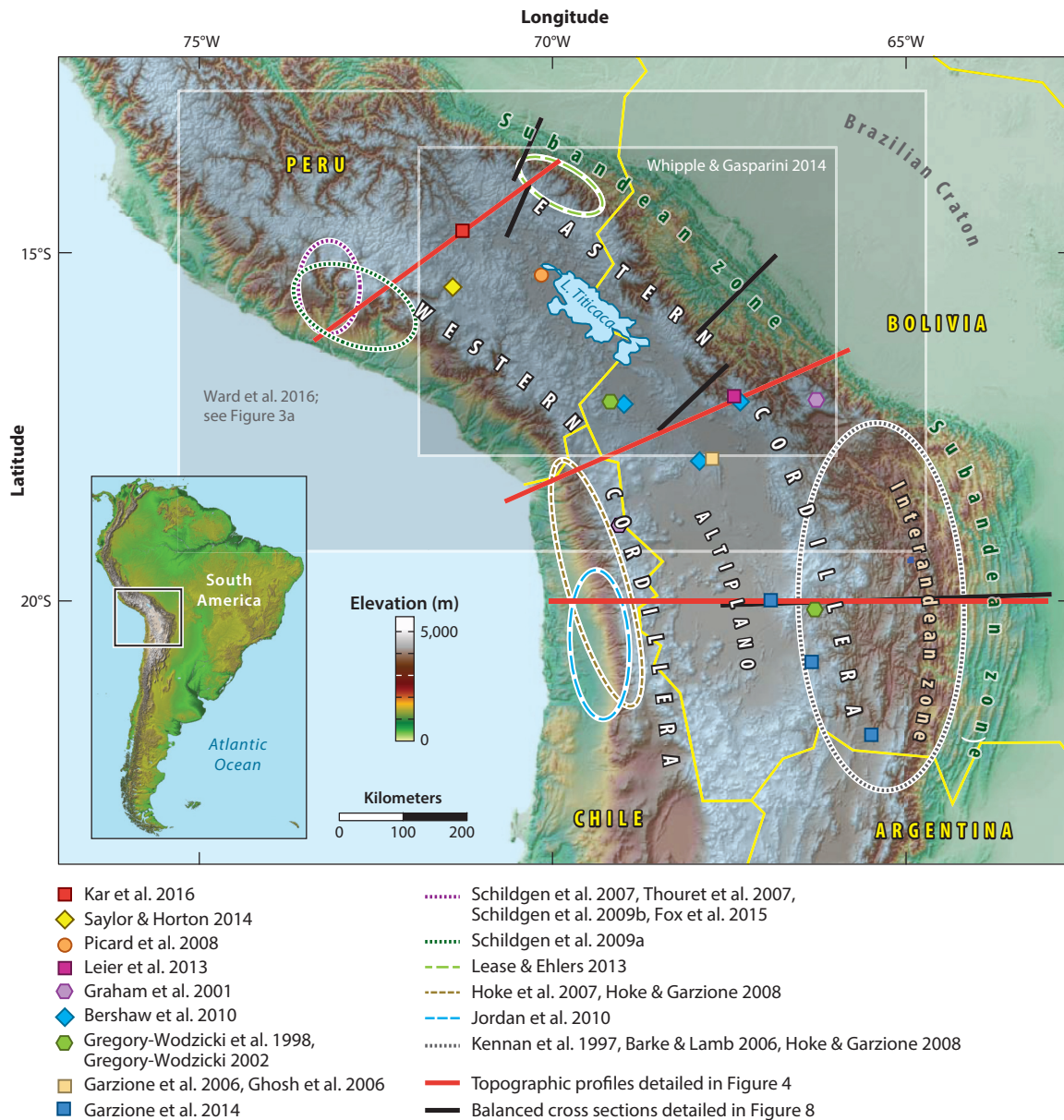
Longitude

75°W 70°W 65°W

Latitude

15°S

20°S

PERU

Whipple & Gasparini 2014

Brazilian Craton

Ward et al. 2016;
see Figure 3a

L. Titicaca

BOLIVIA

South
America

Atlantic
Ocean

Elevation (m)

5,000

0

Kilometers

0   100   200

CHILE   ARGENTINA

- ■ Kar et al. 2016
- ◆ Saylor & Horton 2014
- ● Picard et al. 2008
- ■ Leier et al. 2013
- ⬡ Graham et al. 2001
- ◆ Bershaw et al. 2010
- ● Gregory-Wodzicki et al. 1998, Gregory-Wodzicki 2002
- ▢ Garzione et al. 2006, Ghosh et al. 2006
- ■ Garzione et al. 2014

- ⋯⋯ Schildgen et al. 2007, Thouret et al. 2007, Schildgen et al. 2009b, Fox et al. 2015
- ⋯⋯ Schildgen et al. 2009a
- – – Lease & Ehlers 2013
- – – Hoke et al. 2007, Hoke & Garzione 2008
- – – Jordan et al. 2010
- ⋯⋯ Kennan et al. 1997, Barke & Lamb 2006, Hoke & Garzione 2008
- ── Topographic profiles detailed in Figure 4
- ── Balanced cross sections detailed in Figure 8

Figure 1

Digital elevation map of the Central Andean Plateau showing the locations of other studies referenced in this review.

crustal seismic velocities as well as a variable uppermost mantle with high-velocity material in the uppermost mantle beneath the central part of the Altiplano and low velocities beneath the Eastern Cordillera near the Los Frailes ignimbrite complex (18°–20°S) (Myers et al. 1998, Swenson et al. 1999, Baumont et al. 2002, Beck & Zandt 2002, Heit et al. 2007). Several of these studies concluded that the Brazilian lithosphere has been underthrust westward beneath the Eastern Cordillera, but not beneath the Altiplano (Myers et al. 1998, Beck & Zandt 2002).
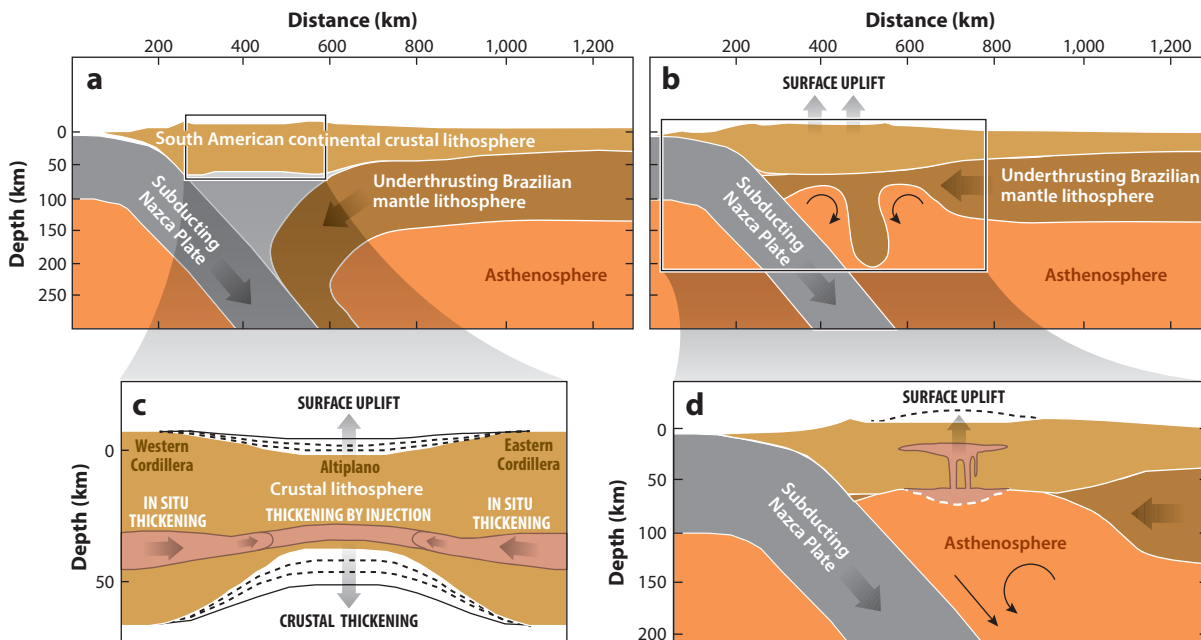
Figure 2

Schematic illustrations of geodynamic processes that may contribute to the surface uplift of orogenic plateaus. (*a*) Ablative subduction of foreland mantle lithosphere associated with protracted crustal thickening and gradual surface uplift (modified from Pope & Willett 1998). (*b*) Rapid removal of a thick portion of dense lower crust (eclogite) and/or mantle lithosphere beneath regions of thickened crust. The region of rapid surface uplift is above the region of thinned lower lithosphere. (*c*) Middle or lower crustal flow from regions of thickened crust to regions of relatively thin crust (modified from Husson & Sempere 2003); shows crustal lithosphere blow-up from panel *a*. Surface uplift occurs in regions where middle to lower crust is thickened by crustal flow. (*d*) Magmatic addition of crustal lithosphere (modified from Perkins et al. 2016); shows blow-up from panel *b*. Pink dashed region shows formation of crustal root from partial melting of mantle asthenosphere after the lower lithosphere removal event. Pink region in middle crust shows batholith formation associated with partial melting of crustal lithosphere. Airy isostatic uplift results from crustal thickening above the region of root formation and batholith emplacement.

In recent years, portable seismic deployments have dramatically increased the number of seismic stations between ~12°S and ~18°S. Studies resulting from the increased seismic coverage along the northern Plateau have imaged thick crust and argue for underthrusting of Brazilian cratonic lithosphere beneath most of the Central Andean Plateau (Phillips et al. 2012, Ma & Clayton 2014). Employing a dense temporary network spanning southernmost Peru and a small area of northwest Bolivia, Phillips et al. (2012) used local tomography and receiver functions to image a mid-crustal (~40 km) discontinuity that they interpreted as the underthrusted Brazilian Shield beneath the entire Altiplano, ending at the Western Cordillera, with no corresponding cratonic mantle root. Each of these studies had a limited aperture, lacking sufficient seismic coverage to resolve structures east of the Eastern Cordillera.

With the aim of investigating the lithospheric structure in the northern Central Andean Plateau, we incorporated an additional 50 broadband seismic stations during a 2-year deployment [CAUGHT (Central Andean Uplift and the Geodynamics of High Topography) deployment] (Beck et al. 2010). These new seismic stations, coupled with nearby permanent and temporary stations (e.g., Wagner et al. 2010), were used to determine crustal thickness over a broad area (Ryan et al. 2016), image the S-wave velocity structure of the lithosphere (Ward et al. 2013, 2016), and locate earthquakes (Kumar et al. 2016).

2.1. Crustal Structure

Ryan et al. (2016) calculated Ps receiver functions using seismic data from the CAUGHT broadband stations, combined with waveforms from 38 other stations in the Bolivian orocline (12°–21°S), to investigate crustal thickness variations. Results from the common conversion point receiver function analysis provide a detailed map of Moho depth relative to sea level that is shown in **Figure 3a**. The active volcanic arc and Altiplano regions have thick crust with Moho depths increasing from the central Altiplano (65 km) to the northern Altiplano (75 km). The Eastern Cordillera shows along strike variations in the Moho depth. Along cross section A-A′ through the Bolivian orocline there is a small region beneath the high peaks of the Eastern Cordillera where the Moho depth varies between 55 and 60 km. By comparison, a broader region of high elevations in the Eastern Cordillera to the south near ∼19°–20°S has a larger Moho depth at ∼65–70 km. Further east beneath the Subandean zone, the Moho depth decreases to ∼40 km (**Figure 3a**).

The surface wave tomography results in **Figure 3c** along the northern cross section A-A' show three main features in the crust: (*a*) a fast forearc crust; (*b*) a significant low-velocity zone under the northern Altiplano basin at a depth of ∼15 km; and (*c*) moderate to low velocities (∼3.4–3.7 km/s) in the middle to lower crust, in particular beneath the Eastern Cordillera. Along the cross section B-B′ (**Figure 3c**), we observe a prominent low-velocity region in the upper 10 km beneath the Altiplano basin, consistent with a thick sedimentary package. Velocities remain low (<3.3 km/s) down to 30 km depth where they merge with similar moderate-to-low, middle to lower crustal velocities, as observed further to the north (**Figure 3c**, cross section C-C′).

2.2. Upper Mantle Structure

The surface wave tomography results (**Figure 3b,c**) show four main features in the upper mantle: (*a*) a positive velocity perturbation associated with the subducting Nazca slab [Nazca slab anomaly (NSA)]; (*b*) a negative velocity perturbation above the slab in the forearc [forearc anomaly (FA)]; (*c*) a negative velocity perturbation above the slab beneath the northernmost Altiplano [slab transition anomaly (STA)]; and (*d*) a high-velocity feature in the mantle above the slab that extends along the length of the Altiplano basin from the base of the Moho to a depth of ∼120 km [sub-Moho Altiplano anomaly (AA)].

Ward et al. (2016) imaged a coherent slab anomaly across most of the model that is consistent with the predicted location of the slab based on earthquake locations (**Figure 3c**). Immediately above the slab and below the forearc in the mantle is a large negative velocity perturbation (FA) with absolute velocities as slow as 3.95 km/s that is likely the serpentinized mantle forearc (**Figure 3b,c**). A similar, but separate and deeper, large negative velocity perturbation in the mantle (STA) is located in the corner, where the Nazca plate transitions from flat to normal subduction (**Figure 3c**). In cross section A-A′, this low-velocity anomaly (versus ∼4.2–4.3 km/s) extends from the volcanic arc in the Western Cordillera to the active Quimsachata volcano in the Eastern Cordillera, between the shallowly dipping Nazca slab at 100 km depth and the base of the ∼65 km thick South American crust. Where the slab dip is steeper further south (cross section B-B′), this low-velocity anomaly is located exclusively beneath the arc and is far less pronounced (versus ∼4.4 km/s) (Ward et al. 2016). To the east we observe a sub-Moho positive velocity anomaly (AA) beneath the Altiplano. In map view at 80 km depth (**Figure 3b**), anomaly AA has a dimension of ∼300 km by 100 km, extending from the base of the crust to ∼120 km depth. A strong spatial correlation exists between the lateral extent of the high-velocity anomaly and relatively lower elevations of the Altiplano basin. The high-velocity anomaly notably does not extend east of the Eastern Cordillera.
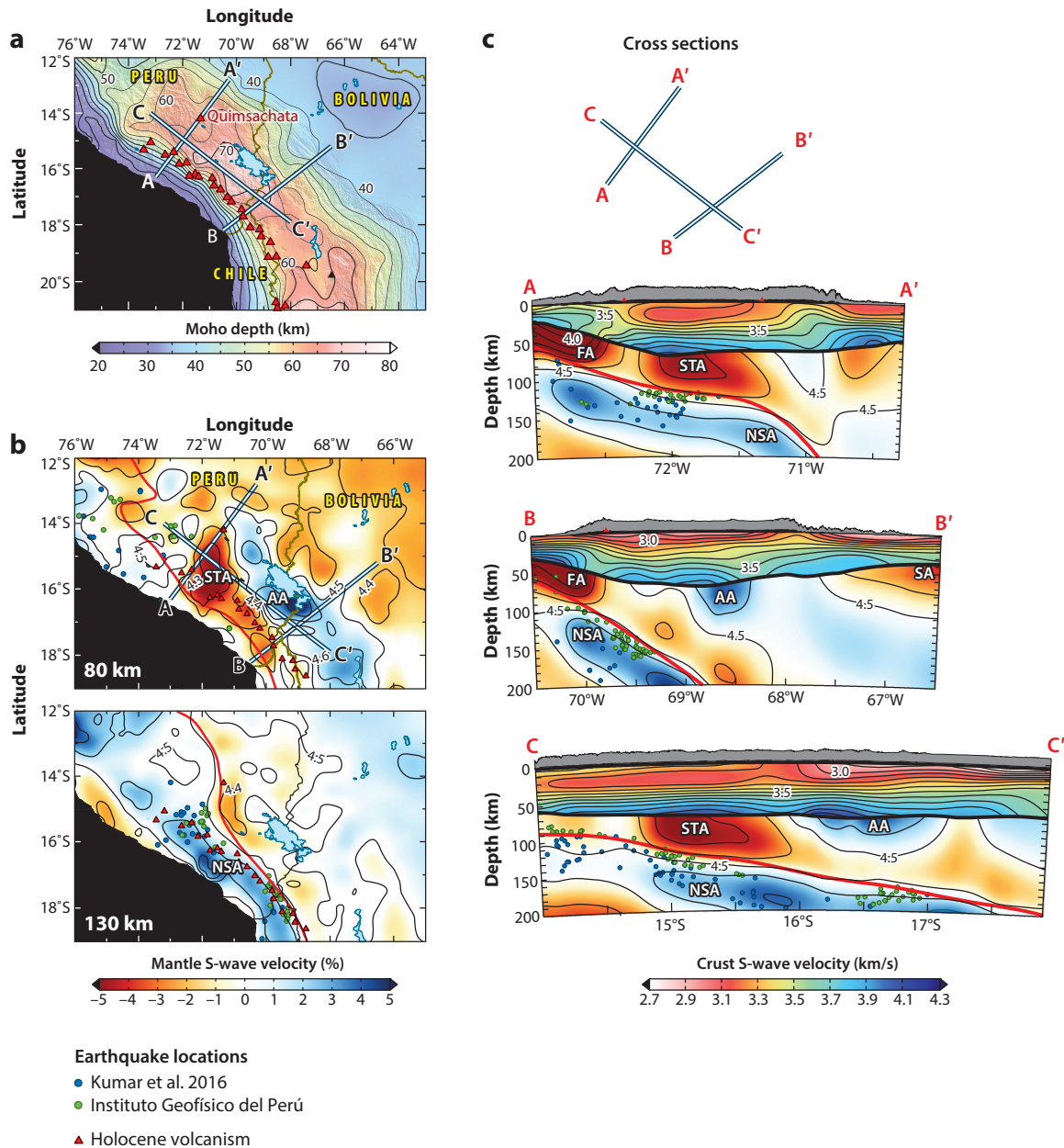
Figure 3

(*a*) Hybrid continental Moho map (relative to sea level) based on depths from Ryan et al. (2016); Tassara & Echaurren (2012); and B.T. Bishop, S.L. Beck, Z. Zandt, M. Long & L.S. Wagner et al. (manuscript in revision). Moho depths are contoured every 5 km with red triangles showing Holocene age volcanism. (*b*) Depth slices at 80 and 130 km from a surface wave tomography study (Ward et al. 2016) based on the joint inversion of ambient noise (Ward et al. 2013) and earthquake-generated surface waves. Slab 1.0 contours (Hayes et al. 2012) are shown as thick red lines, with circles representing earthquake locations from Kumar et al. (2016) (*blue*) and the Instituto Geofísico del Perú (*green*). (*c*) S-wave tomography cross sections shown as perturbations from the starting model in the mantle and absolute velocity in the crust (Ward et al. 2016). In all cross sections, the Moho (from *a*) is shown as a thick black line, and the Slab 1.0 contours (Hayes et al. 2012) are shown as thick red lines. Abbreviations: AA, sub-Moho Altiplano anomaly; FA, sub-Moho forearc anomaly; NSA, Nazca slab anomaly; STA, sub-Moho slab transition anomaly. Figure modified from Ward et al. (2016) with permission.

3. TOPOGRAPHIC EVOLUTION BASED ON PALEOELEVATION STUDIES

The modern day topography (**Figure 4**) of the Central Andean Plateau is characterized by ~5–6 km peak elevations in the Western Cordillera magmatic arc and Eastern Cordillera fold-thrust belt, whereas the Altiplano basin stands at ~4 km. Quantitative paleoelevation estimates of the spatial and temporal evolution of the Central Andean paleotopography have been illuminated through multiple studies (see **Figure 1** for locations and **Supplemental Table 1** for paleoelevation estimates), on the basis of (*a*) reconstructions of the stable isotopic composition of paleometeoric water from $\delta^{18}O$ in sedimentary carbonates and fossil teeth, as well as δD from volcanic glass and leaf waxes (Garzione et al. 2006, 2008; Bershaw et al. 2010; Leier et al. 2013; Saylor & Horton 2014; Kar et al. 2016); (*b*) paleotemperature estimates from Δ_{47} of sedimentary carbonates (Garzione et al. 2006, 2014; Ghosh et al. 2006; Leier et al. 2013; Kar et al. 2016); (*c*) leaf physiognomy paleotemperature estimates and pollen (Gregory-Wodzicki et al. 1998, 2000, 2002; Graham et al. 2001; Kar et al. 2016); (*d*) genetic divergence of a potato parasite nematode (Picard et al. 2008); and (*e*) paleosurfaces and their incision histories (Kennan et al. 1997; Barke & Lamb 2006; Hoke et al. 2007; Schildgen et al. 2007, 2009a,b; Thouret et al. 2007; Hoke & Garzione 2008; Jeffery et al. 2013; Lease & Ehlers 2013; Whipple & Gasparini 2014; Fox et al. 2015) (**Supplemental Table 1**). Using all of these constraints, the reconstructed paleotopography history (**Figure 4**) from different locations in the Western Cordillera, Eastern Cordillera, and Altiplano basin reveals that the Cenozoic evolution of the Central Andean Plateau is marked by considerable variation in the nature and timing of surface uplift, both along and perpendicular to the strike of the plateau.

An assumption of all paleoelevation proxies is that the observations represent an uncorrupted record of elevation change. Recent work using paleoclimate models has demonstrated that this assumption is not always valid because elevation histories are calculated using modern climate conditions and often uncorrected for past climate conditions. In particular, climate change associated with surface uplift during mountain building and global climate change may obscure the signals used to interpret elevation change (Ehlers & Poulsen 2009, Poulsen et al. 2010, Poulsen & Jeffery 2011, Insel et al. 2012, Jeffery et al. 2012, Feng et al. 2013, Fiorella et al. 2015, Feng & Poulsen 2016). **Figure 5** illustrates this point with simulated annual precipitation rates, temperature, and amount-weighted precipitation $\delta^{18}O$ for Andean surface uplift from 40% to 80% and 100% of modern elevations. In these three cases, annual Altiplano precipitation rates, temperature, and $\delta^{18}O$ change are approximately 100–200, 300–400, and 600–700 cm/day; 20–22, 14–16, and 8°–10°C; and −5, −7, and −10‰ (**Figure 5**). The results demonstrate a changing stable isotope versus elevation relationship with changing climate fields and surface elevation. An increase in surface elevation from 80% to 100% of modern elevations produces similar or larger climate changes than increases from 40% to 80% of modern elevations—twice the elevation change. The results in **Figure 5** are not model dependent and have been demonstrated here using the ECHAM global model and in previous studies using the GENESIS (Poulsen et al. 2010), REMO (Insel et al. 2012), and RegCM (Insel et al. 2010) models. Unless accounted for, climate change can lead to errors in the interpretation of paleoelevation by hundreds of meters to several kilometers (e.g., Poulsen et al. 2010, Insel et al. 2012, Feng et al. 2013, Fiorella et al. 2015). The principal challenge to correcting paleoelevation estimates for climate change associated with surface uplift is that the surface elevation is unknown. Recent studies of paleoelevation proxies attempt to address this challenge by applying climate change "corrections" associated with the effects of surface uplift on climate (Leier et al. 2013, Garzione et al. 2014, Kar et al. 2016) on the basis of modeling studies (Ehlers & Poulsen 2009, Insel et al. 2012).
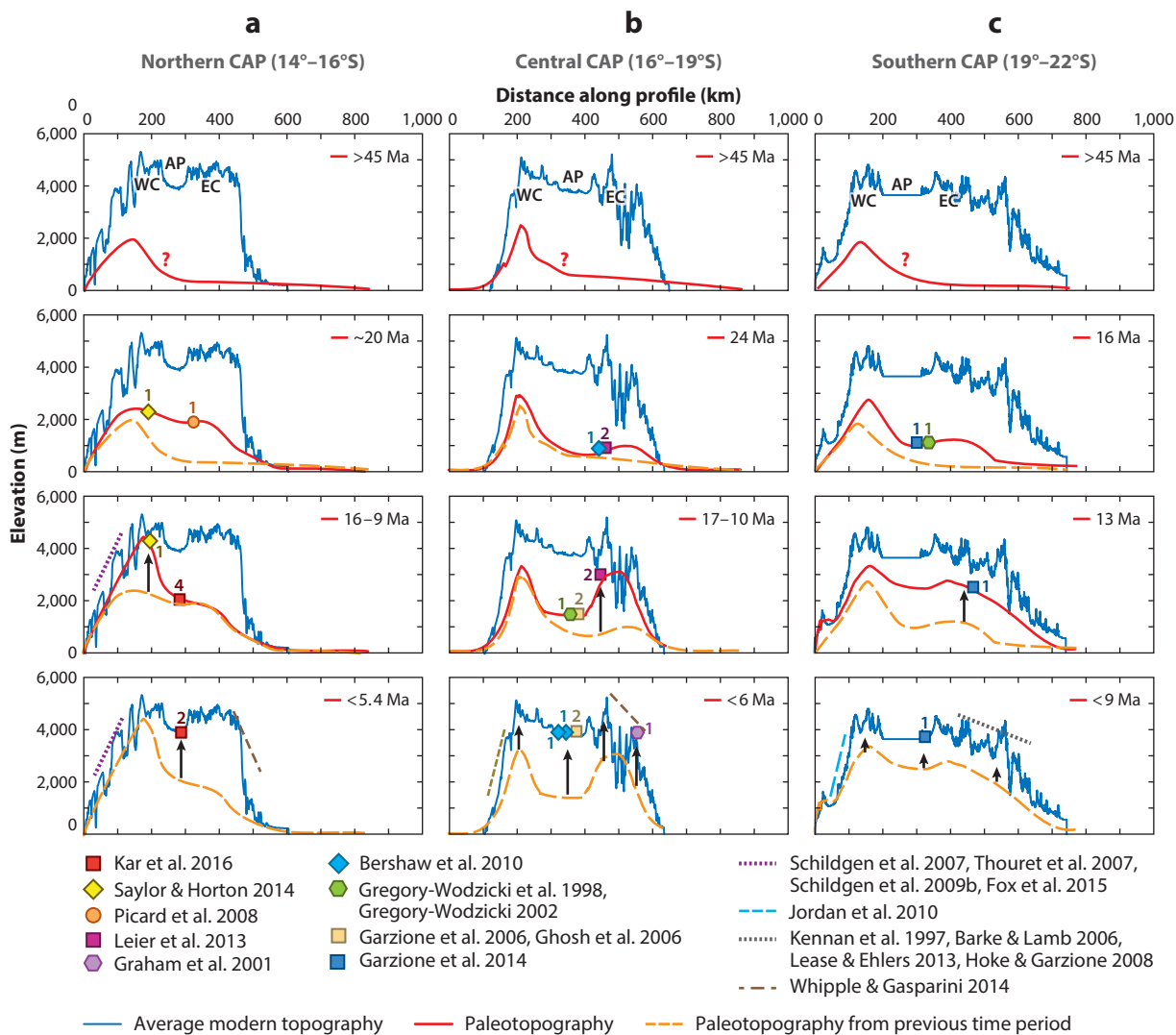
Figure 4

Schematic illustrations of paleotopographic evolution along transects in the northern (*a*), central (*b*), and southern (*c*) Central Andean Plateau (CAP). Location of elevation transects are shown as red lines in **Figure 1**. Red curves show schematic representation of paleotopography for each time period; orange dashed curves show paleotopography from the previous time period, with the area between curves representing the magnitude of surface uplift between time periods. Red question marks denote time periods for which there are no paleoelevation proxy records, and inferred elevation is speculative. Paleoelevation sites (symbols shown in **Figure 1**) are projected along strike onto each topographic profile for the time period studied. Numbers show the number of different proxies per study site. See **Figure 8a–c** for plots of paleoelevation over time for the EC and AP. Paleotopography is drawn using the highest elevation (most conservative) end-member estimates where multiproxy estimates exist. Black arrows denote rapid (>0.5 km/Myr) pulses of surface uplift discussed in the text. Thick dashed lines of various colors denote surface uplift inferred from studies of river incision; regions are shown in **Figure 1**. Abbreviations: AP, Altiplano; EC, Eastern Cordillera; WC, Western Cordillera.
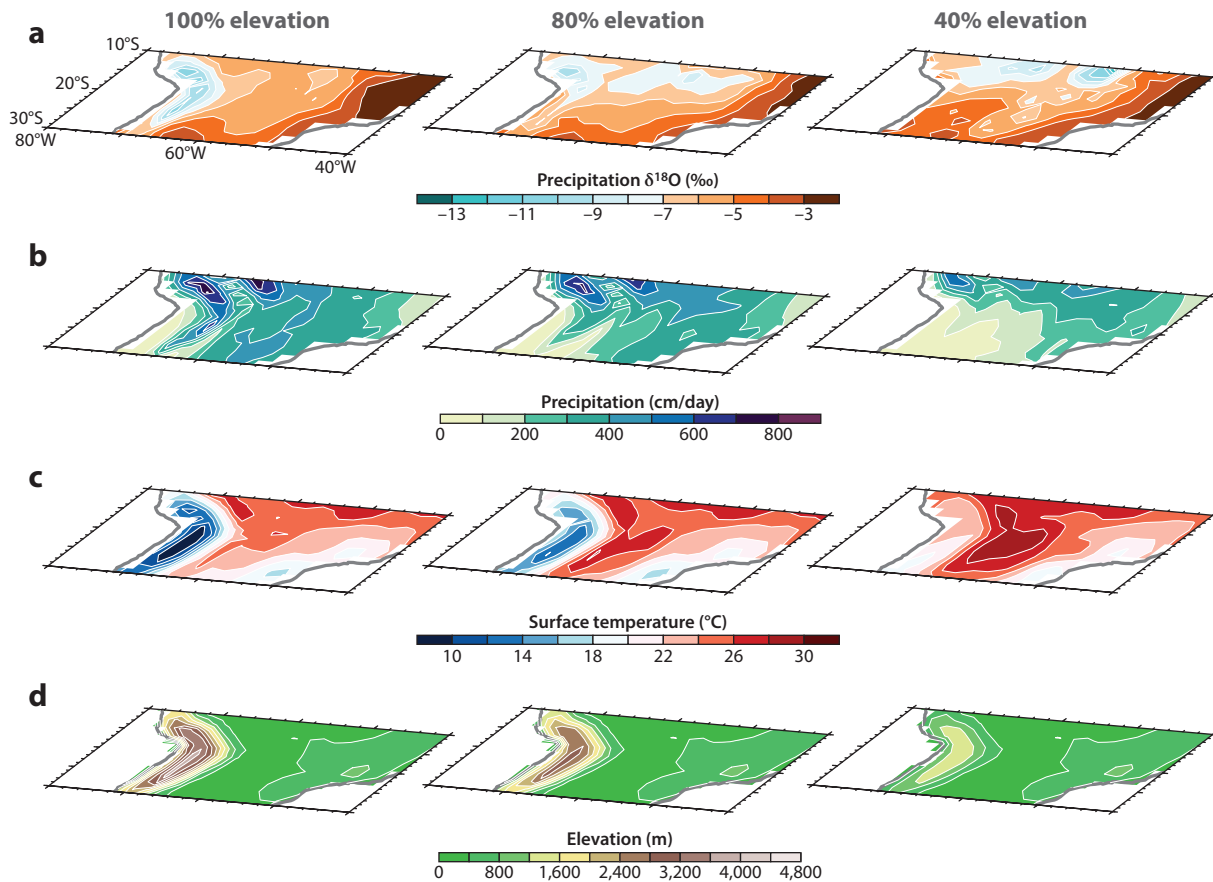
Figure 5

Simulated responses to Andean elevations for three cases with elevations of 100%, 80%, and 40% of modern elevation. Mean-annual (*a*) amount weighted precipitation $\delta^{18}O$ (‰), (*b*) precipitation (cm/day), (*c*) surface temperature (°C), and (*d*) elevation (m). Simulations were performed with an isotope-enabled global climate model, ECHAM5-wiso. All boundary conditions (e.g., greenhouse gas concentrations, surface vegetation, sea-surface temperatures) other than elevation are the same between cases and equivalent to modern values. The responses to elevation illustrated in *a–c* include the direct elevation response (attributed to lapse rate effects) and climate response effects (typically neglected in proxy interpretations). Note that the responses are nonlinear and not limited to regions of elevation change.

Here, we report the most conservative paleoelevation estimates that account for uplift-related climate change and show the higher elevation end-member where multiproxy estimates exist (**Figure 4**).

The Paleocene–middle Eocene depositional history of the northern part of the Central Andean Plateau shows that accumulation took place at sea level within the Altiplano–Eastern Cordillera region (Carlotto 2013). At this time, deposition also began throughout the central and southern Altiplano in an early foreland basin setting that formed due to the topographic load of an incipient mountain belt to the west (Horton et al. 2001). Early surface uplift (>45 Ma) of the Western Cordillera (**Figure 4**) is inferred on the basis of magmatic arc activity and associated thickening of the crustal lithosphere, as well as the presence of a Paleocene–Eocene foreland basin within the Altiplano. Although the early elevation history of the Western Cordillera is not well constrained,

paleoelevation estimates from δD of felsic volcanic glass show that the Western Cordillera of southern Peru achieved a minimum paleoelevation of 250 m and a maximum of ∼2 km in the early Miocene (19 Ma) and reached the modern elevation of 4.5 km by 16 Ma (Saylor & Horton 2014) (**Figure 4a**). West of this region, Schildgen et al. (2009b) determined canyon incision of up to 3 km between ∼11 and 2.2 Ma in the Western Andean Escarpment that coincided with or postdated surface uplift of the Western Cordillera. However, an analysis of incision of the Peruvian Ocoña canyon, which accounted for changes in precipitation amount due to surface uplift, demonstrated that river incision places loose constraints on the timing and rates of surface uplift (Jeffery et al. 2013). Comparison between the surface uplift history of the Western Cordillera determined from δD of volcanic glass (Saylor & Horton 2014) and river incision (Schildgen et al. 2009b) indicates an ∼5-Myr lag time between surface uplift and canyon incision.

Early surface uplift (∼45 to 20 Ma) of the Eastern Cordillera (**Figure 4**) is inferred on the basis of crustal thickening histories discussed in Section 6. However, stable isotope ($\delta^{18}O$ and Δ_{47})–based paleoelevation reconstruction from the Eastern Cordillera (Bershaw et al. 2010, Leier et al. 2013) indicates that paleoelevation was low (0–1 km) until latest Oligocene–early Miocene, followed by surface uplift of ∼2.5–3 km between 24 and 17 Ma (**Figure 4b**).

The Altiplano shows diachronous surface uplift that occurred between middle Miocene and early Pliocene time. In the northern Altiplano basin, a multiproxy-based paleoelevation reconstruction using pollen, δD of leaf wax, $\delta^{18}O$ of paleosol carbonate and Δ_{47} of paleosol, lacustrine, and palustrine carbonate (Kar et al. 2016) suggests that the Altiplano remained at an elevation of 1–2 km until 9 Ma, and reached the modern day elevation of ∼4.2 ± 0.9 km (2σ) by 5.4 Ma, approximately 9 ± 2 Ma after the Western Cordillera in this region rose to its full height (**Figure 4a**). Rapid canyon incision dated at 4–3 Ma along the northeast plateau margin of the Peruvian Eastern Cordillera (Lease & Ehlers 2013) reflects a 1–2-Myr lag between surface uplift of the Altiplano (Kar et al. 2016) and incision of the northeast plateau margin.

A similar pattern of surface uplift has also been documented in the central Plateau (∼16°–19°S; **Figure 4b**). In the Altiplano basin, elevation histories from plant physiognomy (Gregory-Wodzicki et al. 1998, 2000, 2002) and stable isotope ($\delta^{18}O$ and Δ_{47}) studies (Ghosh et al. 2006; Garzione et al. 2006, 2008) provide surface uplift estimates of 2.5 ± 1 km between 10 and 6 Ma that brought the Altiplano to its modern elevation of ∼4 km. This timing is consistent with an additional pulse of surface uplift of ∼2–3 km in the Eastern Cordillera, estimated on the basis of river incision histories of regional low-relief paleosurfaces beginning after ∼9–12 Ma (Barke & Lamb 2006, Whipple & Gasparini 2014). Graham et al. (2001) calculated a surface uplift of 2.3 ± 1.1 km between 7 and 6 Ma from pollen and spore records. Whipple & Gasparini (2014) used river profile analysis of the northern-central Eastern Cordillera to propose a ∼3 km surface uplift within the past 12 Myr. Reconstructed ∼10 Ma paleotopography (Hoke & Garzione 2008) from paleosurfaces on both the eastern and western flanks of the Plateau suggests that both the Western Cordillera and Eastern Cordillera experienced surface uplift over the same time period as the Altiplano, implying an orogen-wide event.

In comparison, paleoelevation estimates from the southern part (∼19°–22°S) of the Central Andean Plateau indicate that modern elevations were reached notably earlier than in the northern-central Central Andean Plateau (**Figure 4c**). Clumped isotope records (Garzione et al. 2014) suggest ∼2.6 ± 0.7 km surface uplift between 16 and 9 Ma that established the modern Altiplano elevation, with most of that surface uplift occurring between 16 and 13 Ma. An approximately −5‰ decrease in the $\delta^{18}O$ values of southern foreland paleosols starting at 12 Ma suggests increased rainfall due to growing hinterland topography (Mulch et al. 2010). Aridity trends measured from the Atacama Desert paleosols (Rech et al. 2006) argue for the initiation of hyperaridity between 19 and 13 Ma, a timeframe that overlaps with proposed initial surface uplift of the southern

Central Andean Plateau. These studies point to an older age of onset of rapid surface uplift in the southern Altiplano Plateau that preceded the central-northern Plateau by $7 \pm 4\,\text{Myr}$, highlighting a diachronous nature of surface uplift along-strike in the Central Andean Plateau (**Figure 4**).

4. PETROLOGIC CONSTRAINTS ON LITHOSPHERIC EVOLUTION

Andean arcs are composed chiefly of intermediate magmas (tonalite to granodiorite) and contain relatively minor amounts of mafic material (gabbro and ultramafic cumulates; Mamani et al. 2010; Ducea et al. 2013, 2015a). Approximately 50% of the mass composing the arc is derived from melting of the convective mantle wedge above subducting slabs, with the remainder being derived from the continental mantle lithosphere and lower crust (Ducea et al. 2015b). The balance between lithospheric and asthenospheric material can be deduced from whole rock radiogenic isotopic ratios, such as $^{143}\text{Nd}/^{144}\text{Nd}$. Geochemical ratios, such as Sr/Y and La/Yb, correlate with crustal thickness as shown in modern arcs around the globe including the Andes (Turner & Langmuir 2015, Chapman et al. 2015) and can be used to track regional variations in crustal thickness over time (Profeta et al. 2015). Furthermore, rare xenoliths transported to the surface via small volumes of Pliocene to Quaternary potassic to ultrapotassic lavas (e.g., Carlier et al. 2005, Thouret et al. 2007, Chapman et al. 2015) provide direct constraints on the composition of the upper plate crust. These lavas are found 100 km or more inboard from the active frontal arc volcanoes and are referred to as "back arc" rocks. Here, we discuss magma chemistry and lower crustal xenolith-based constraints on the evolution of crustal thickness of the Central Andean Plateau, with emphasis on the northern part of the Plateau because data from the southern Plateau are sparse (**Figure 6**).

The Late Cretaceous marks a significant change in character of Central Andean Plateau magmatism. Prior to this time, mafic volcanic and intrusive suites were emplaced into thin crust in an extensional regime. In the Late Cretaceous, intermediate to felsic continental arc magmas indicate the onset of contractional deformation at ~90 to 80 Ma, evidenced by angular unconformities and intrusive relationships along the Western Cordillera (Mégard 1984, Haschke & Guenther 2003, Scheuber & Reutter 1992, Maksaev et al. 1988).

Trace element ratios sensitive to crustal thickness [e.g., Sr/Y, La/Yb, and other (REE) ratios; **Figure 6**] (Chiaradia 2015, Profeta et al. 2015, Turner & Langmuir 2015) evolve over time from baseline values typical of relatively thin (<40 km) crust to those reflecting a continental arc with a developing residual mafic keel (>40 km; Mamani et al. 2010). These geochemical proxies indicate a slow rate of crustal thickening into the early Eocene (Mamani et al. 2010). Arc magmatism and contractile deformation migrated inboard in the early Eocene (Carlotto 2013), possibly in response to shallowing of the subducting oceanic plate (Sandeman et al. 1995, James & Sacks 1999). This shallowing of the subduction angle resulted in hydration of the upper mantle (James & Sacks 1999; Wagner et al. 2005, 2006; Kay & Coira 2009).

Associated with this change, geochemical proxies show an increased rate of crustal thickening from late Eocene through early Miocene (45–20 Ma) (**Figure 6**). Metasedimentary xenoliths from Quaternary back-arc volcanic centers in southern Peru corroborate evidence for Eocene thickening. A suite of felsic granulite xenoliths of inferred first-cycle (Paleozoic and Triassic) sedimentary origin, recovered with a suite of mafic meta-igneous xenoliths, yield garnet Sm-Nd ages of ~42 Ma, suggesting that metamorphism associated with burial of these rocks from the surface to ~30–35 km paleodepths occurred in Eocene time (McLeod et al. 2013, Chapman et al. 2015). The presence of these probable Mitu Formation equivalents at >30 km depth under the northernmost Altiplano requires significant shortening in the Eastern Cordillera prior to 42 Ma as well as a significant amount (>10 km) of magmatic thickening (Chapman et al. 2015). This period of crustal thickening corresponds to the jump in locus of deformation from the Western
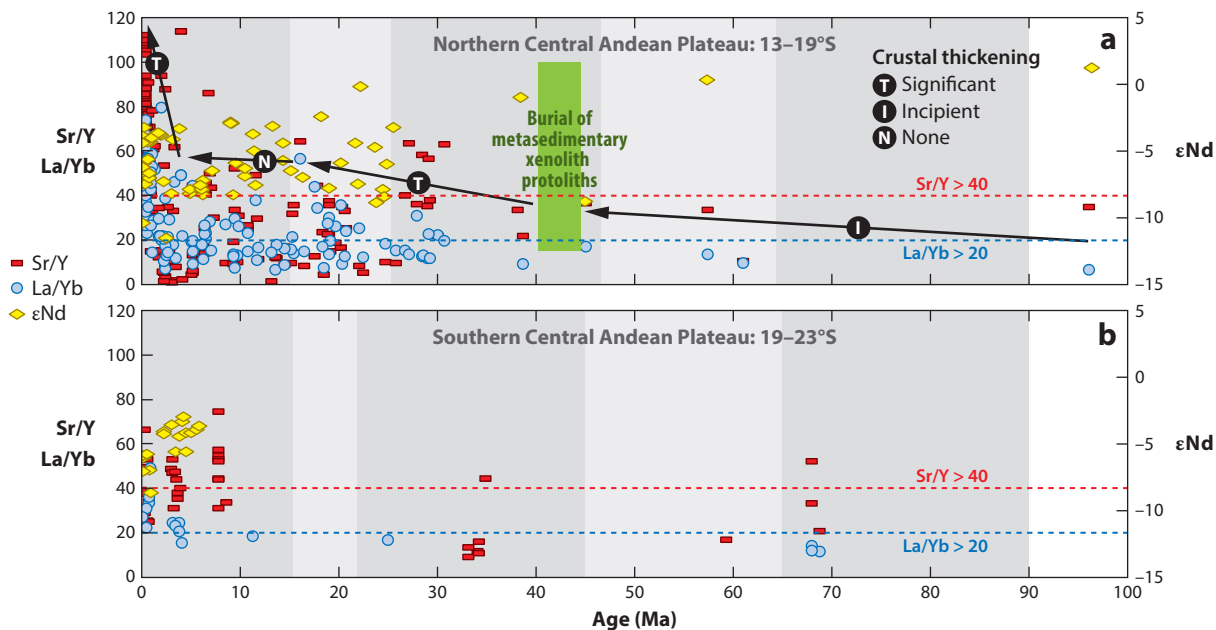
Figure 6

Summary of petrologic evidence for crustal thickening beneath the (*a*) northern and (*b*) southern Central Andean Plateau. Xenolith geochronologic constraints from Chapman et al. (2015). Trace element (Sr/Y and La/Yb) and Nd isotopic values from Mamani et al. (2010), Profeta et al. (2015), and M.N. Ducea & A.D. Chapman (manuscript under review). Black arrows in panel *a* show inferred periods of significant crustal thickening (T), incipient thickening (I), and no significant thickening (N), based on increasing Sr/Y and La/Yb values with time. Note dashed lines indicating Sr/Y and La/Yb threshold values. Lavas yielding Sr/Y and La/Yb values greater than 40 and 20, respectively, are inferred to reflect melting of garnet-rich and plagioclase-poor residue (Ducea et al. 2015b). For the average composition of the Central Andean arc, the garnet-in and plagioclase-out transition takes place over a depth range of 40–60 km at temperatures above 800°C. Timing of crustal shortening (*gray bands*) from Mégard (1984); Maksaev et al. (1988); Farrar et al. (1988); Kontak et al. (1990); Sempere et al. (1990); Scheuber & Reutter (1992); Lamb & Hoke (1997); Haschke & Guenther (2003); McQuarrie et al. (2005, 2008); Gillis et al. (2006); Uba et al. (2009); Perez et al. (2016a,b). Lighter gray indicates periods of shortening inferred from foreland basin formation and migration (60–45 Ma) or decreased shortening rates (25–15 Ma).

Cordillera into the Eastern Cordillera initiating at ~50–45 Ma (McBride et al. 1987; Farrar et al. 1988; Kontak et al. 1990; Sempere et al. 1990; Lamb & Hoke 1997; McQuarrie et al. 2005, 2008; Gillis et al. 2006; Carlotto 2013; Perez et al. 2016a,b).

Following a ~10-Myr interval of relative magmatic quiescence from ~40 to 30 Ma, the proposed flat subducting slab began to steepen, leading to widespread volcanism as cold oceanic lithosphere was replaced by upwelling, hot asthenosphere-promoting crustal melting (Sandeman et al. 1995, Allmendinger et al. 1997, James & Sacks 1999, Oncken et al. 2006, Mamani et al. 2010). Consistent with this scenario, lavas erupted during the early Oligocene portion of this steepening episode not only have geochemical signatures indicative of derivation from the mantle, but also show an increasing signal of crustal melting and assimilation with time (Sandeman et al. 1995, Mamani et al. 2010). The resumed magmatism accompanies a marked slowing in shortening rates (Gillis et al. 2006, McQuarrie et al. 2008, Rak 2015) and modest increase in crustal thickness based on geochemical proxies (Sandeman et al. 1995, Mamani et al. 2010).

Magma composition remained relatively constant across the northern Central Andean Plateau arc from middle to late Miocene time, suggesting that crustal thickness did not change significantly during this time (Mamani et al. 2010). However, starting at ~20 Ma—associated with the eastward

sweep in magmatism—εNd values evolved gradually to more negative values, indicating an influx of crustal material (DeCelles et al. 2009).

Geochemical parameters in the northern Central Andean Plateau magmatic arc (southern Peru) suggest significant crustal thickening in Pliocene and Quaternary time (Mamani et al. 2010; Profeta et al. 2015; M.N. Ducea & A.D. Chapman, manuscript under review; **Figure 6**), following large magnitude surface uplift that was completed by ~5 Ma (Kar et al. 2016).

5. ALTIPLANO BASIN EVOLUTION

Composite Cenozoic basin fill (>7 km) in the Altiplano spans the transition from a foreland to hinterland setting in response to deformation and volcanic arc processes. Early Paleocene lacustrine and distal fluvial deposits in Bolivia have eastern sources (Horton et al. 2001), whereas late Paleocene–early Oligocene coarse sandstones and conglomerates deposited in fluvial and alluvial fan settings were sourced mainly from western arc sources (Carlotto 2013; Horton et al. 2002, 2015). Eocene fold-thrust belt structures in the Western Cordillera of southern Peru are obscured by Neogene volcanic rocks; however, they are coeval and likely correlative with the east-vergent Marañon fold-thrust belt of central Peru (Mégard 1984, Carlotto 2013) (**Figure 7a**). Paleocene–lower Oligocene deposits from the Altiplano are interpreted as backbulge, proximal foredeep, and wedge-top foreland basin fill, with subsidence driven by an eastward migrating fold-thrust belt in the Western Cordillera.

The volcanic arc of the northern-central Plateau advanced eastward beginning at ~45 Ma (Mamani et al. 2010), simultaneously with the abrupt shift in deformation to the bivergent Eastern Cordillera fold-thrust belt (**Figure 7a**) (Sempere et al. 1990, McQuarrie et al. 2005, Carlotto 2013). Continued eastward migration of the magmatic arc between 30 and 24 Ma is synchronous with backthrust motion along the Altiplano-Eastern Cordillera margin fault zone as constrained by ~28–26 Ma growth strata with attendant rapid sedimentation in the Altiplano basin (**Figure 7b**) (Sempere et al. 1990, Carlotto 2013, Perez & Horton 2014, Horton et al. 2015). Provenance records from clastic deposits reveal a late Oligocene transition to Eastern Cordillera sources, demonstrating that encroaching Eastern Cordillera deformation controlled the evolution of the Altiplano basin (Murray et al. 2010, Perez & Horton 2014). By Oligocene time, the Altiplano was an active hinterland basin situated between the Western Cordillera arc and Eastern Cordillera fold-thrust belt (Horton et al. 2002, Horton 2012) (**Figure 7a,b**).

The volcanic arc began migrating trenchward at ~24 Ma (**Figure 7c**), associated with generally finer-grained deposits in the Altiplano basin within smaller fluvial networks and isolated lacustrine/palustrine environments. Sediment accumulation rates decreased by up to an order of magnitude, and provenance data indicate competing Eastern Cordillera and Western Cordillera sediment contributions from the Altiplano margins. Coarse alluvial fan deposits containing intraformational angular unconformities and ~17–16 Ma growth strata reveal localized, out-of-sequence hinterland deformation (Perez & Horton 2014, Kar et al. 2016), in contrast to regionally extensive Eocene–Oligocene shortening. Contemporaneous fine-grained hinterland deposition, diminished accumulation rates, and spatially distributed deformation were coincident with rapid Western Cordillera uplift at ~17 Ma (Saylor & Horton 2014). Similarly, surface uplift of the northernmost Altiplano between ~9 and 5.4 Ma (Kar et al. 2016) and the central Altiplano between ~10 and 6 Ma (Garzione et al. 2006) (**Figure 7d**) is associated with a change in hinterland basin deposition from coarse poorly organized fluvial systems to fine-grained lacustrine/palustrine and well-organized fluvial systems, as well as an order of magnitude decrease in sediment accumulation rates (Garzione et al. 2008). In the Descanso-Yauri basin of the northernmost Altiplano, late Miocene surface uplift is also associated with the cessation of shortening and onset of minor
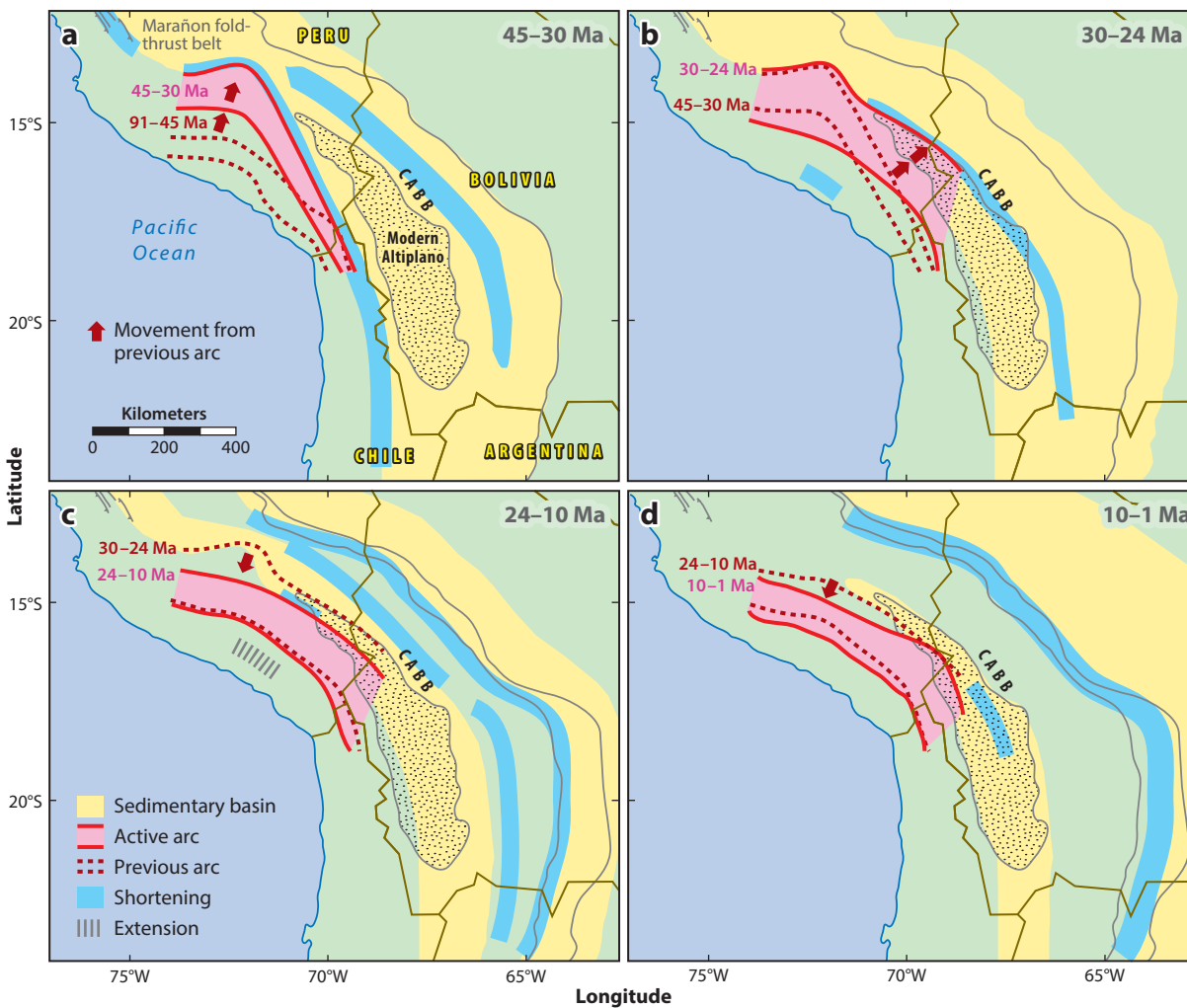
Figure 7

Four-part coevolution of basin deposition (*yellow shading*), shortening location (*light blue shading*), and volcanic arc position (*red outline/pink shading*) for (*a*) 45–30 Ma, (*b*) 30–24 Ma, (*c*) 24–10 Ma, and (*d*) 10–1 Ma. Stippled region shows the modern Altiplano basin. Red arrows show movement direction from previous arc location (*dark red dashed line*). Deformation location and timing: Mégard (1984, 1987); Farrar et al. (1988); Sempere et al. (1990); Gubbels et al. (1993); Barnes et al. (2006); Gillis et al. (2006); Schildgen et al. (2009a); Murray et al. (2010); Lamb (2011); Perez & Horton (2014). Magmatic arcs: Sandeman et al. (1995), Mamani et al. (2010), Demouy et al. (2012). Central Andean backthrust belt (CABB): McQuarrie & DeCelles (2001). Marañon fold-thrust belt: Mégard (1978), Farrar et al. (1988). Modified from Horton et al. (2015).

▶Erratum

normal faulting (Kar et al. 2016). Continued trenchward motion of the late Miocene and younger magmatism was coeval with these events (**Figure 7d**).

6. CRUSTAL SHORTENING AND THICKENING HISTORY

A growing number of studies have applied low-temperature thermochronology techniques, such as apatite (U-Th)/He and zircon (U-Th)/He (respectively, AHe and ZHe) dating; apatite-fission track and zircon-fission track (respectively, AFT and ZFT) dating; and $^{40}Ar/^{39}Ar$ dating of

muscovite and feldspar, tied to balanced structural cross sections, to provide information on the timing and rates of Central Andean growth. Integration of structural, thermochronometric, and paleoclimate data provides insights into the age of deformation in the central Andes assuming that cooling is driven by erosional exhumation in response to deformation and the growth of structural relief (e.g., Ehlers 2005).

The earliest deformation history of the Central Andes (80–50 Ma) is marked by the formation of structures (Chong 1977, Maksaev et al. 1988, Scheuber & Reutter 1992, Cobbold et al. 2007), significant vertical-axis rotations (Arriagada et al. 2003, Roperch et al. 2006), and basin development (Coney & Evenchick 1994, Mpodozis et al. 2005, Arriagada et al. 2006) along the outer forearc to the modern volcanic arc. The magnitude of shortening at this time is unknown, although shortening estimates range from ∼30 km to >200 km (Scheuber & Reutter 1992, McQuarrie et al. 2005). The eastward jump in the fold-thrust belt from the Western Cordillera to the Eastern Cordillera is recorded by AFT, ZHe, ZFT, and $^{40}Ar/^{39}Ar$ thermochronologic data that show rapid cooling of rocks from 50–20 Ma, consistent with initial shortening-related exhumation in the Eastern Cordillera at ∼45 ± 5 Ma (**Figure 8**) (Benjamin et al. 1987; McBride et al. 1987; Farrar et al. 1988; Kontak et al. 1990; Barnes et al. 2006, 2008, 2012; Scheuber et al. 2006; McQuarrie et al. 2008; Gillis et al. 2006; Eichelberger et al. 2013).

Between 29 and 24 Ma, synorogenic sediments buried structures in the Eastern Cordillera (Sempere et al. 1990, Kay et al. 1998, Gillis et al. 2006, Leier et al. 2010, Perez & Horton 2014). Slowing in the rate of exhumation at ∼25–20 Ma indicates that most deformation had migrated eastward toward the Interandean Zone and Subandean Zone. The majority of AFT samples within the northern-central (15°–17°S) Eastern Cordillera of Bolivia have young cooling ages (<20 Ma; ∼60 ages total), indicative of rapid cooling initiating at ∼15–11 Ma (Benjamin et al. 1987; Barnes et al. 2006, 2012; Gillis et al. 2006; Safran et al. 2006; McQuarrie et al. 2008). This young exhumation continued northward into Peru where ∼15 Ma ZHe ages and ∼4–3 Ma AHe ages record rapid cooling at these times (Lease & Ehlers 2013, Perez et al. 2016b).

Similar to the Eastern Cordillera, AFT cooling ages in the Interandean Zone also include both young (∼15–10 Ma) and old (∼40–30 Ma) ages, indicating protracted, two-phase cooling. However, the cooling history of the Subandean Zone has been harder to ascertain. Model-constrained cooling of thrust sheets in the Subandean Zone using AFT data suggest that accelerated cooling initiated 19–4 Ma, with the most rapid cooling at 12–5 Ma (Barnes et al. 2006). AHe and ZHe cooling ages and thermal history inverse modeling refine Subandean Zone cooling and document rapid cooling initiation in northern Bolivia at 6 ± 2 Ma, and in southern Bolivia at 11 ± 3 Ma (Lease et al. 2016). In Peru, three AHe samples from the Subandean Zone are partially to fully reset, requiring the onset of deformation and associated exhumation by 6 ± 3 Ma, although possibly as early as 15 Ma (Perez et al. 2016b).

Shortening recorded by numerous surface folds and faults in the Central Andes must be accompanied by equal magnitudes of shortening in basement rocks, with differing proposed geometries for basement deformation (Kley 1996, Baby et al. 1997, McQuarrie 2002, Müller et al. 2002, McQuarrie et al. 2008, Gotberg et al. 2010, Eichelberger et al. 2013, Perez et al. 2016b). Different basement geometries have predictable effects on surface geometries, kinematics, and mineral cooling ages (McQuarrie et al. 2008; McQuarrie & Ehlers 2015, 2017). The geologic cross sections that we present (**Figure 8**) show two stacked basement thrust sheets, with the higher thrust sheet underlying the Eastern Cordillera (**Figure 8**, green shading). As this upper basement thrust moved, smaller scale folds and faults in the sedimentary rocks exposed in the Eastern Cordillera and Interandean Zone were shortened by the same amount (123–218 km; see McQuarrie 2002, McQuarrie et al. 2008, Eichelberger et al. 2013, Perez et al. 2016b), and were raised by the basement thrust sheet. The 50–20 Ma cooling ages observed across the Eastern Cordillera and into the
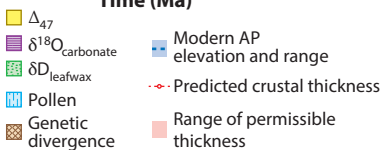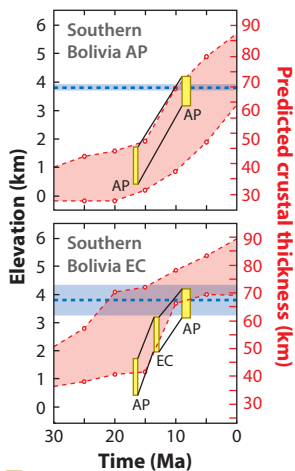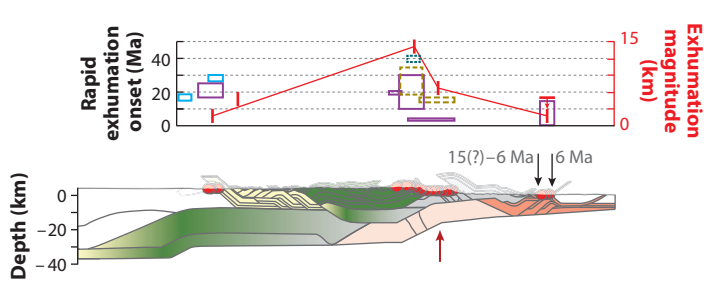
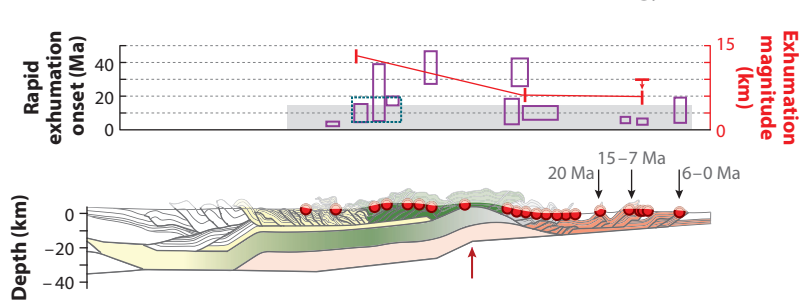**a** Northern Andean Plateau (14–16°S)
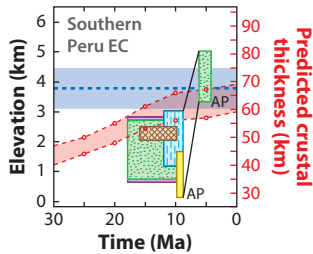
b Central Andean Plateau (16–19°S)
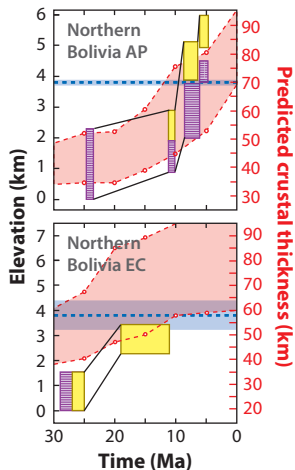
c Southern Andean Plateau (19–22°S)

d Northern Peru cross section and thermochronology

15(?)–6 Ma   6 Ma

e Central (northern Bolivia) cross section and thermochronology

20 Ma   15–7 Ma   6–0 Ma

f Southern (southern Bolivia) cross section and thermochronology

14 Ma   11 Ma   2 Ma

Legend:
- Δ_{47}
- $\delta^{18}O_{carbonate}$
- $\delta D_{leafwax}$
- Pollen
- Genetic divergence
- Modern AP elevation and range
- Predicted crustal thickness
- Range of permissible thickness
- Growth strata
- Apatite (U-Th)/He
- Zircon (U-Th)/He
- Ar/Ar or K/Ar
- Age of deformation front
- Active uplift region
- Thermochronology samples
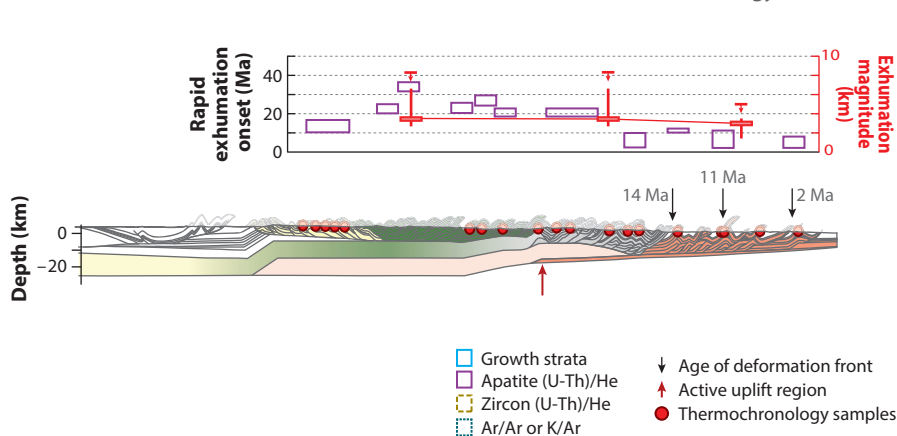
Interandean Zone are interpreted to reflect exhumation driven by vertical motion on footwall and hanging wall ramps that is associated with eastward motion of the upper basement thrust sheet (McQuarrie et al. 2005, 2008; Barnes et al. 2008; Eichelberger et al. 2013; Perez et al. 2016a,b).

The onset ages for Subandean Zone deformation of the 6 ± 2 Ma for the northern Bolivian and 11 ± 3 Ma for the southern Bolivian Subandean Zone (Lease et al. 2016) are based on both regional patterns of Subandean Zone cooling ages versus sample depths and modeled thermal histories for individual samples. Whether these ages indicate initiation of deformation is uncertain. Subandean deformation is linked to a lower basement thrust sheet (**Figure 8**, pink shading) that feeds shortening into the sedimentary rocks exposed in the Subandean Zone and passively uplifts and facilitates erosion of the rocks exposed in the Interandean Zone (Kley 1996; McQuarrie 2002; McQuarrie et al. 2008; Eichelberger et al. 2013; Perez et al. 2016a,b). Both 10–14 Ma AFT cooling ages in the Interandean Zone (Barnes et al. 2006, McQuarrie et al. 2008) and 7–9 Ma synorogenic sedimentary deposits that overlie deformed and eroded Ordovician rocks (Mosolf et al. 2011) suggest an earlier start for Subandean Zone deformation. Additional rock uplift and exhumation occur on the footwall ramp of this basement thrust sheet (**Figure 8**, red arrow), providing a mechanism by which to drive the rapid and young (∼12–5 Ma) exhumation recorded in the Eastern Cordillera samples, particularly in northern Bolivia (Whipple & Gasparini 2014, Rak 2015). Other explanations for this period of recent rapid cooling in the Eastern Cordillera include an increase in precipitation tied to the Eastern Cordillera reaching >75% of its modern elevation at 15–11 Ma (Barnes et al. 2012) and/or a pulse of rapid incision into the arid, high-elevation plateau in the past 4 Myr (Lease & Ehlers 2013).

Different scenarios for Central Andean Plateau elevation histories have implications for deformation of the adjacent Subandean Zone. Rapid elevation gain or elevation crossing a critical threshold would cause the orogenic wedge of the Andes to be supercritical and promote propagation and deformation into the Subandean Zone to increase the length of the wedge to lower its taper. Thus, a young 10–6 Ma (northern Bolivia) or 16–13 Ma (southern Bolivia) increase in elevation would promote deformation and the young pulse of exhumation (6 ± 2 Ma in the

← ───

Figure 8

Timing comparison of predicted crustal thickening (*red circles*) and paleoaltimetry data (*patterned boxes*) by region for (*a*) northern, (*b*) central, and (*c*) southern Central Andean Plateau. The axes are scaled so modern crustal thickness and mean modern Altiplano (AP) elevation (∼3.8 km) are colinear (*thick blue dashed line* indicates average while lighter blue shading indicates range). Pink shaded region between red dashed lines indicates the range of permissible thickness depending on an initial crustal thickness of 40 km (*upper limit*) or 35 km (*lower limit*). (*a*) Northern AP paleoelevation estimates from Kar et al. (2016). In the central Eastern Cordillera (EC) (*b*), large standard deviations in predicted thickness are due to concentration of excess thickness along the western edge of the EC, spatially coincident with paleoaltimetry data (Leier et al. 2013). Central AP: paleoaltimetry estimates from Garzione et al. (2006), and Ghosh et al. (2006), revised by Garzione et al. (2014). (*c*) Southern EC and AP paleoaltimetry estimates from Garzione et al. (2014). Note that AP results are shown on the EC plot for comparison to single EC paleoelevation sites. Representative balanced cross sections and thermochronology sample locations from (*d*) northern (Peru), (*e*) central (northern Bolivia), and (*f*) southern (southern Bolivia) regions of the central Andean Plateau. Cross sections shown in panels *d*, *e*, and *f* are shown in **Figure 1** as black lines. Cross sections are shown at equivalent scales and color-coded based on the physiographic zones and age of deformation. Interpreted basement faults in each section are also color coded according to the age and magnitude of basement faulting and surface shortening. The lower basement thrust (*pink shading*) balances shortening in the Subandean Zone, whereas the upper basement thrust (*green shading*) balances shortening in the Interandean Zone and EC. The positions of thermochronology samples are shown by red dots. References for each section: panel *d*, Perez et al. (2016a,b); panel *e*, McQuarrie et al. (2008); panel *f*, McQuarrie (2002), Barnes et al. (2008). Above each cross section are graphs that describe mineral cooling ages (*colored rectangles*) and exhumation magnitude (*vertical red bars* and associated *red lines*). Horizontal red lines with arrows pointing down indicate the maximum limit of exhumation based on unreset thermochronometers. Black arrows above cross section indicate age and location of deformation front (Uba et al. 2009; Rak 2015; Lease et al. 2016; Perez et al. 2016a,b), and red arrow beneath profile points to the top of the ramp in the modern fault surface that is collocated with the region of active uplift, exhumation, and young cooling ages.

north and 11 ± 3 Ma in the south) in the Subandean Zone (Garzione et al. 2006, 2008; DeCelles et al. 2009; Lease et al. 2016). In contrast, linking this young exhumation in the northern Bolivian Eastern Cordillera and Interandean Zone to the basement thrust sheet associated with Subandean Zone shortening requires that Subandean Zone shortening initiated between 18 and 12 Ma, significantly earlier than the 6 ± 2 Ma pulse of rapid cooling documented in the northern Bolivian Subandean Zone; the rapid cooling in this scenario would indicate the latest motion on the thrust sheets that brought those rocks to the surface.

7. INTEGRATION AND IMPLICATIONS FOR MECHANISMS FOR OROGENIC PLATEAU GROWTH

Each hypothesized geodynamic mechanisms for the growth of orogenic plateaus has an associated set of predictable geologic observations. Evaluation of the processes that have built the Central Andean Plateau requires an understanding of the surface uplift history as it relates to modern crustal and lithospheric structure and the geologic evolution of the lithosphere. **Table 1** summarizes how geologic observations summarized here contribute to evaluation of various geodynamic processes responsible for plateau growth. We emphasize that crustal thickening associated with shortening is necessary for building an orogenic plateau. One question addressed here is, What is the role of shortening in determining the timing of surface uplift of the Plateau? Another question is, By what process is the lower crustal and mantle lithosphere removed beneath the Plateau? For example, is gradual surface uplift coincident with crustal shortening, thereby requiring ablative subduction of foreland mantle lithosphere beneath the shortening mountain belt (**Figure 2a**)? Or, does shortening result in the accumulation of lower crust and mantle lithosphere, along with heating and weakening of the lower lithosphere, that ultimately leads to periodic removal of lower lithosphere (**Figure 2b**)? A comparison of the crustal thickening history based on balanced cross section reconstructions and surface uplift history (**Figure 8a–c**) enables assessment of whether punctuated removal of lower lithosphere (**Figure 2b**) and lower crustal flow (**Figure 2c**) is allowable given the time evolution of crustal thickening and the timing and rates of surface uplift. For example, if predicted crustal thickness exceeds modern values at the time of rapid surface uplift, then removal of high-density lower crustal material is implicated; if predicted crustal thickness falls short of modern values at the time of surface uplift, then lower crustal flow is suggested. If crustal thickening occurs at the same time as surface uplift, then neither removal of high-density lower lithosphere nor crustal flow is required, and ablative subduction of the lower lithosphere may have occurred. The following discussion is focused on various time slices in the tectonic evolution of the Central Andean Plateau where significant geologic events allow for inferences of likely geodynamic processes.

7.1. Modern Crustal and Mantle Lithosphere Structure

Seismic imaging techniques are well-suited for determining modern structures in the crust and mantle from which inferences on their genesis may be drawn. In the origin of the Central Andean Plateau, there are two areas on which seismology sheds light: (*a*) the role of lithospheric removal in the observed elevation history and (*b*) the role of mid or lower crustal flow in the redistribution of crustal material. In both cases, the modern structures provide some end-member guidance but do not provide definitive proof of any one hypothesis due to the inability to know how these structures evolved over time from the seismology alone.

In the central Plateau region near 19°–20°S, Myers et al. (1998) imaged low-P-wave velocities in the mantle beneath the Eastern Cordillera that could indicate a region of lower lithospheric

Table 1   Expected observations in evaluating different geodynamic mechanisms for growth of the Central Andean Plateau

	Ablative subduction of foreland mantle lithosphere	Foundering or convective removal of lower lithosphere	Lateral flow of middle to lower crustal material	Magmatic addition of crustal material
Geophysical characteristics of the crust	Thick crust with preserved high-velocity lower crust	Variable thickness felsic crust lacking high-velocity lower crust	Laterally continuous middle to lower crustal low velocity zone	Crustal low-velocity zone localized over regions of high-magmatic flux
Geophysical characteristics of the mantle	Heterogeneous and high upper mantle seismic velocities and low attenuation, with westward subducting geometry for foreland lithosphere; LAB identification under high elevations	Low upper mantle seismic velocities and high Vp/Vs ratios; high attenuation consistent with asthenosphere; LAB missing under the high elevations (i.e., no mantle lithosphere detected)	NA	NA
Surface uplift history	Gradual surface uplift; rate reflects crustal shortening rates	Rapid surface uplift decoupled from the crustal shortening history	Rapid surface uplift during time periods of crustal thickening that are decoupled from the crustal shortening history	Rapid surface uplift during time periods of crustal thickening associated with high-magmatic flux
Petrology and geochemistry of magmas	Trace element ratio evidence for gradual crustal thickening that is paced with shortening (not definitive)	High-magmatic flux with upper plate isotopic signatures during and immediately following removal, followed by increases in ϵ_{Nd} and decreases in $^{87}Sr/^{86}Sr$ associated with mantle-derived melts after removal	Trace element ratio evidence for rapid crustal thickening in the absence of shortening and magmatic addition	Trace element ratio evidence for rapid crustal thickening during high-magmatic flux and in the absence of shortening
Kinematic history	Progressive outward growth and change in the locus of fold-thrust belt deformation; crustal thickness balanced with shortening history	Outward jump in locus of shortening associated with removal events; shortening history predicts crustal thickening in excess of modern thickness	Modern crustal thickness exceeds that which can be accounted for by shortening history	Modern crustal thickness exceeds that which can be accounted for by shortening history and is localized around regions of extensive magmatism
Exhumation and river incision history	Exhumation tracks crustal shortening history (not definitive)	Exhumation tracks both shortening and surface uplift histories; phases of removal of lower lithosphere would cause exhumation in the absence of crustal shortening	Exhumation tracks both crustal thickening and surface uplift histories in the absence of shortening	NA

Abbreviations: LAB, lithosphere–asthenosphere boundary; NA, not available; Vp/Vs, P-wave to S-wave velocity ratio.

removal. This could help to explain the late Miocene surface uplift of the Eastern Cordillera in the central Plateau.

We see clear evidence for the presence of mantle lithosphere and/or eclogitized lower crust beneath the comparatively low elevations of the Altiplano basin (AA anomaly; **Figure 3**). Although this indicates that the mantle lithosphere was not removed entirely during a foundering event, we cannot determine, based on seismology alone, if the mantle was thicker or more laterally extensive in the past. We note, however, that the strong correlation between the location of the modern mantle lithosphere and the lower elevations of the Altiplano basin suggests that the two may be causally related. This relationship could be explained if the existing mantle lithosphere were in the process of foundering.

Adjacent to this mantle lithosphere, we see a pronounced low-velocity anomaly in the mantle beneath the northwesternmost Central Andean Plateau (STA anomaly; **Figure 3**). This low-velocity anomaly could be the signature of a past lithospheric removal event, but its location at the southern edge of the Peruvian flat slab allows for an additional alternate interpretation. Recent anisotropy studies suggest that trench parallel flow above the normally subducting Nazca plate may be deflected to the northeast parallel to the flat slab contours (Antonijevic et al. 2015; Long et al. 2016). This flow, together with the likely accumulation of water or melt, could explain the replacement of high-velocity mantle lithospheric material with low-velocity hydrous or partially molten mantle. The slow anomaly beneath the northernmost Altiplano (STA) is therefore likely caused in part by the southward advance of the Peruvian flat slab, which would make it a relatively young feature (1–2 Ma; Antonijevic et al. 2015). If this is correct, it could help explain the presence of the relatively young volcanism observed by Chapman et al. (2015).

Flow in the middle or lower crust cannot be directly imaged seismically. The moderate to low velocities we observe in the middle and lower crust across much of the Central Andean Plateau are consistent with, but not uniquely indicative of, the reduced shear strength that would be a necessary condition for flow to occur.

7.2. Middle Miocene to Pliocene Time

Surface uplift appears to be diachronous along strike in the Altiplano and Eastern Cordillera over this time frame, with the earliest pulses in the southern Altiplano between ~16 and 13 Ma younging to late Miocene and early Pliocene in the central and northern Plateau, respectively (**Figures 4** and **8**). A comparison of the crustal thickening and surface uplift histories (**Figure 8a–c**) enables assessment of whether removal of high-density lower crust and lower crustal flow are allowable given the pace of thickening and surface uplift.

7.2.1. Southern Plateau (19°–22°S). Figure 8c shows that southern Altiplano and Eastern Cordillera crustal thickening occur over the same 16 to 9 Ma time frame as surface uplift in the Altiplano. Predicted crustal thicknesses remain lower than the modern mean values and therefore do not require that high-density lower crustal material, such as eclogite, was removed. Taking the mean thickness estimated for the Altiplano region of 44 km and 57 km at 16 Ma and 9 Ma, respectively, and assuming foreland mantle lithosphere is continuously removed by ablative subduction, crustal thickening alone can produce an isostatic surface uplift of 2.4 km[1] over this time frame, similar to Garzione et al.'s (2014) estimates of 2.6 $\pm$ 0.7 km. However, if mantle lithosphere

---

[1]The Isostasy calculation assumes a mantle density of 3.3 g/cm^3 and crustal density of 2.7 g/cm^3.

thickens and accumulates at the same rate as crustal thickening, then minimal surface uplift would result from crustal thickening, requiring an additional mechanism for surface uplift.

Although the comparison of crustal thickening and surface uplift histories allows for either continuous removal or punctuated removal of lower lithosphere during the middle–late Miocene in the southern Central Andean Plateau, several other geologic indicators, discussed below, are consistent with rapid surface uplift by lower lithosphere removal (**Table 1**). Deformation of the Andean fold-thrust belt propagated eastward in the middle–late Miocene (∼15–5 Ma) (McQuarrie et al. 2005, Uba et al. 2009, Echavarria et al. 2003), causing rapid exhumation of the Subandean Zone by 11 ± 3 Ma (Lease et al. 2016). According to critical taper theory, this lengthening of the fold-thrust belt could have resulted from attainment of a supercritical tapered wedge (Horton 1999) by flexural unloading of the rear of the fold-thrust belt when dense lower lithosphere was detached (Garzione et al. 2006). In addition, climate changes to hyperarid conditions on the western slope of the Andes between 19 and 13 Ma (Rech et al. 2006) and wetter conditions in the Subandean foreland beginning at ∼12 Ma (Mulch et al. 2010) are both consistent with general circulation model simulations of the climate response to a rising plateau (Poulsen et al. 2010, Insel et al. 2012). Surface uplift of the southern Western Cordillera over the same time frame as the Altiplano, evidenced by rotation of paleosurfaces, suggests 0.8 ± 0.6 km of surface uplift between 11 and 5 Ma, followed by 0.4 ± 0.2 km since the late Miocene (Jordan et al. 2010). The simultaneous increase in both Altiplano and Western Slope elevation implicates a regional geodynamic process, such as the removal of lower lithosphere.

7.2.2. Central Plateau (16°–19°S). The central Plateau (**Figure 4b**) shows low-relief paleosurfaces throughout the Eastern Cordillera that are dated at ∼12–10 Ma and represent an equilibrium landscape that formed at a time when the Eastern Cordillera was much lower (2–3 km) (Barke & Lamb 2006, Whipple & Gasparini 2014). Deep incision of these surfaces over the past ∼10 Ma has been interpreted as the response to rapid surface uplift of the central Plateau between ∼10 and 6 Ma (Hoke & Garzione 2008) (**Figure 4b**). Geomorphic analyses of the northern extent of these surfaces (18°–14°S) also indicate that surface uplift continued from 6 Ma to present and is ongoing today (Gasparini & Whipple 2014, Whipple & Gasparini 2014), and/or that incision increased as a result of late Pliocene global climate change with enhanced moisture transport to the region (Jeffery et al. 2013, Lease & Ehlers 2013). On the Western Slope of the central and southern Plateau, fluvial incision of low relief paleosurfaces starting between 10 and 5.4 Ma suggests 1,100 ± 200 m of surface uplift of the Western Cordillera (Hoke et al. 2007) over the same time frame as Altiplano surface uplift and the onset of incision in the Eastern Cordillera, suggesting orogen-wide surface uplift (**Figure 4b**).

The crustal thickening history of the central Central Andean Plateau suggests only moderate thickening of the Altiplano over the late Miocene from a mean thickness of 60 km at 10 Ma to 65 km at 6 Ma. Thickening of the Altiplano lithosphere from 60 to 65 km can only produce 0.9 km of surface uplift assuming Airy isostatic balance, insufficient to account for the 2.5 ± 1 km surface uplift estimated from a range of proxies for this time period (**Figure 4b**). One way to reconcile this difference is via a high-density lower lithospheric root that held the surface down prior to 10 Ma and detached between 10 and 6 Ma. Alternatively, thinner initial crust and delayed addition of crustal material via crustal flow would also produce a thickening history that would closely match the measured surface uplift history (**Figure 8**). Thus, the elevation and thickening history can be reconciled through either removal of lower lithosphere or crustal flow between 10 and 6 Ma.

If crustal flow is responsible for late Miocene surface uplift of the central Altiplano, then crustal material could have been derived from the southern Plateau, which began to rise earlier than the central Altiplano, or from the central Eastern Cordillera, which has a large excess of

crustal material [derived from shortening estimates (Eichelberger et al. 2015; **Figures 4b,c** and **8b,c**)]. Crustal flow from the southern Plateau toward the central Altiplano is unlikely because thickening in the central Plateau exceeds that in the south. Alternatively, the higher elevation and greater thickness (**Figures 4b** and **8b**) of the central Eastern Cordillera, in addition to continued shortening, may have provided the gravitational potential energy to drive westward flow from the Eastern Cordillera to the Altiplano. To explain the surface uplift record of the Altiplano via lower crustal flow from the Eastern Cordillera, an additional uplift mechanism is required to account for the simultaneous elevation increase in the Eastern Cordillera. Both Barke & Lamb (2006) and Whipple & Gasparini (2014) proposed that shortening along a crustal scale ramp (**Figure 8**, red arrows) would provide an ongoing mechanism for Eastern Cordillera uplift.

Multiple lines of geologic evidence lend support to a combination of removal of lower lithosphere and lower crustal flow to generate late Miocene surface uplift of the central Plateau (**Table 1**). Evidence supporting lower lithosphere removal comes from the 6 ± 2 Ma age of exhumation in the northern Bolivian Subandean Zone (Lease et al. 2016), inferred to reflect propagation of deformation into the Subandean Zone. However, work in progress (McQuarrie et al. 2015, Rak 2015) that incorporates thermochronometry data in a thermal and structural restoration of the thrust belt suggests onset of the northern Bolivian Subandean Zone deformation is earlier (18–14 Ma), with predicted cooling ages matching measured ages in the Interandean Zone and Eastern Cordillera associated with uplift on the basement ramp (Rak 2015; **Figure 8**). Additional support for lower lithosphere removal beneath the Altiplano–Eastern Cordillera border comes from observation of modern low-P-wave velocities in the mantle beneath this region (see Section 7.2) and the eruption of the Morococala ignimbrite complex between 9 and 5 Ma (Kay & Coira 2009 and references therein), similar to the age of most of the Los Frailes complex in the southern Plateau. If the trigger for crustal melting that generates ignimbrites is related to heating by lower lithospheric removal (Kay & Coira 2009), this suggests removal prior to 9 Ma. In addition, the crustal heating and melting required to generate large-volume ignimbrites supports lower crustal flow as a viable mechanism for Altiplano uplift (Kay & Coira 2009). We therefore suggest that both lower lithosphere removal and crustal flow from the Eastern Cordillera to the Altiplano account for some portion of the large-magnitude, late Miocene surface uplift of the Altiplano and the redistribution of excess crustal thickness within the central Eastern Cordillera (**Figure 8b**).

7.2.3. Northern Plateau (14°–16°S). The northern Altiplano rose from a moderate paleoelevation of ≤2 km to its modern elevation between 9 and 5.4 Ma over a similar, if slightly younger, time frame as the central Altiplano (Kar et al. 2016; **Figures 4a** and **8a**). Unlike the central and southern Plateau, studies of the shortening budget of the northern Plateau (Gotberg et al. 2010; Perez et al. 2016a,b) show that shortening cannot account for the modern crustal thickness (**Figure 8a**), suggesting thickening mechanisms, such as magmatic addition and/or middle to lower crustal flow (**Figure 2b,c**; **Table 1**). The predicted thickening history of the Eastern Cordillera from balanced cross sections (**Figure 8a**) shows minimal thickening over the time frame of Altiplano surface uplift. In sharp contrast, trace element ratios of crustal melts suggest thickening over the past 5 Ma (**Figure 6**), slightly postdating evidence for surface uplift. Although there is a lag time between geochemical evidence for crustal thickening and the timing of surface uplift, we infer that thickening in the absence of shortening can be accounted for by either magmatic addition or crustal flow. In the northern plateau, rapid surface uplift of ≥2 km at ~17–16 Ma in the Western Cordillera may have provided the gravitational potential energy to drive eastward crustal flow and rapid uplift of the Altiplano. Similarly, a thickened and high-elevation central Plateau could have provided crustal material for northward flow (**Figures 4a,b** and **8b**). The moderate

to low velocities observed in the middle and lower crust across the Central Andean Plateau are consistent with material capable of flow (Ward et al. 2013).

The extent to which magmatic thickening contributes to rapid rates of surface uplift in the Central Andean Plateau is less clear than the contributions of middle to lower crustal flow. A region in which there is well-documented evidence for surface uplift by magmatic addition is the Altiplano-Puna Volcanic Complex (APVC) at ∼21.5°–23.5°S. This region has experienced high-flux ignimbrite volcanism since ∼11 Ma, associated with an imaged magma body at 10–20 km depth that has generated a 1 km topographic dome at the surface (Perkins et al. 2016). If magmatic addition is responsible for Pliocene–present crustal thickening in the northern Plateau, high-flux volcanism and surface doming are not obvious features as in the APVC.

There is also evidence for lower lithosphere removal in the northern Altiplano of Peru. Kar et al. (2016) documented the sedimentary and deformation history of the Descanso-Yauri basin during the time period of Altiplano surface uplift. As the Altiplano rose from ∼1–2 km at ∼9 Ma to ∼4 km by 5.4 ± 1 Ma, shortening ceased within the basin, and minor normal faulting followed. Plateau surface uplift after 9 Ma is also associated with a cessation in sedimentation that resulted in an erosional unconformity between ∼9 and 5.4 ± 1 Ma. Both the cessation in sediment accumulation and the transition from shortening to extension in the Descanso-Yauri basin are consistent with observations from "bobber basins" (DeCelles et al. 2015a,b) that are modeled as forming above regions of lower lithosphere removal (Wang et al. 2015). S-wave tomography of the mantle beneath the northwestern Altiplano shows a large low-velocity anomaly (STA) (**Figure 3b,c**; Ward et al. 2016), consistent with hot asthenosphere. The geometry of this anomaly, together with anisotropy results, suggests that its current low velocities are likely due to the southward progression of the Peruvian flat slab. However, we cannot rule out an earlier episode of lithospheric removal in this area that contributed to the observed surface uplift. Chapman et al. (2015) report Pliocene-recent mantle melts and asthenospheric derived xenoliths in the northern Altiplano that support inferences of a recent lower lithosphere removal event.

7.3. Late Oligocene to Early Miocene Time

The Eastern Cordillera within the Central Andean Plateau region, with its protracted crustal thickening history (McQuarrie et al. 2005, 2008; Eichelberger et al. 2015) and lack of high-density crustal and mantle lithospheric root (Beck & Zandt 2002, Ward et al. 2016), is the strongest candidate for lower lithospheric removal. Portions of the Altiplano retain thin (∼120 km deep) roots of high-velocity material (**Figure 3**, AA anomaly) that are associated with slightly lower elevations (≤500 m; e.g., Titicaca region) compared to surrounding regions. The Eastern Cordillera, however, lacks this remnant high-velocity material. In the central Eastern Cordillera, crustal thickening predictions based on balanced cross section reconstructions (**Figure 8b**) show that Eastern Cordillera thickening dramatically exceeds modern crustal thicknesses, requiring crustal flow from the Eastern Cordillera into surrounding low-lying regions and/or the removal of high-density lower crust, such as eclogite. Comparing the crustal thickening predictions with the surface uplift history of the Eastern Cordillera reveals that crustal thicknesses first exceeded modern thickening in early Miocene time, immediately preceding the time period of inferred rapid surface uplift of the Eastern Cordillera between 24 and 17 Ma (Leier et al. 2013; **Figures 4b** and **8b**). This surface uplift event was coincident with an eastward magmatic sweep and widespread ignimbrite eruptions over the modern width of the Central Andean Plateau (Allmendinger et al. 1997, Mamani et al. 2010). The observations that the Eastern Cordillera accumulated crustal thickness early but remained at low elevations and rose rapidly after shortening in the region had ceased (Leier et al. 2013) support the removal of eclogitic lower crustal and mantle lithosphere as the process that

caused surface uplift (Eichelberger et al. 2015) (**Table 1**). Additional evidence for lower litho-sphere removal comes from a seismically imaged decrease in Moho depth of ∼10 km beneath this region (Eichelberger et al. 2015, Ryan et al. 2016; **Figure 3***b*). The significance of the magmatic sweep and ignimbrite flare-up across the plateau in the context of removal of lower lithosphere is less clear. James & Sacks (1999) proposed that volcanic quiescence in the 10 Myr leading up to the flare-up was associated with flat slab subduction, and the magmatic sweep resulted from steepen-ing of the subducting slab. Regardless of the exact cause of the ignimbrite flare-up, it is clear that heating of the crustal lithosphere occurred over the same time period as surface uplift. Further evidence to support the removal of lower lithosphere is provided by the widespread (∼1,000 km^2) eruption of the Tambo Tambillo basaltic and shoshonitic volcanics between ∼25 and 22 Ma in the central Plateau region, with REE compositions that suggest derivation from shallow mantle depths of <90 km (Lamb & Hoke 1997).

8. SUMMARY

This review of the lithospheric evolution and surface uplift of the Central Andean Plateau provides insights into the geodynamic mechanisms that grow broad, high-elevation orogenic plateaus and highlights regions that have likely experienced rapid removal of lower lithosphere and crustal thick-ening by middle to lower crustal flow and magmatic addition. In particular, we document a spatially and temporally punctuated history of Plateau surface uplift. We point to the latest Oligocene–early Miocene and late Miocene pulses of surface uplift of the central Eastern Cordillera as showing evidence for multiple lower lithosphere removal events beneath the Central Andean Plateau in the same location. Lines of supporting geologic evidence for this include crustal thicknesses that exceed modern thickness and multiple episodes of ignimbrite eruptions associated with crustal heating that are closely followed by mafic volcanism sourced from mantle asthenosphere. We suggest that late Miocene lower lithosphere removal was accompanied by structural growth on a crustal scale ramp and middle-lower crustal flow from the central Eastern Cordillera to the Altiplano and to the northern Central Andean Plateau.

The northern Central Andean Plateau provides an example of punctuated late Miocene to Pliocene surface uplift via mid to lower crustal flow and/or magmatic addition processes, possibly following a lower lithosphere removal event. We demonstrate that crustal shortening cannot account for the modern crustal thickness of this region and point to the magmatically thickened northern Western Cordillera and structurally thickened central Eastern Cordillera as potential sources for middle to lower crustal material. Both of these regions experienced earlier pulses of surface uplift at 17–16 Ma and 10–6 Ma, respectively, that would have provided the gravitational potential energy to drive crustal flow toward the northernmost Plateau.

DISCLOSURE STATEMENT

ACKNOWLEDGMENTS

Author affiliations are as follows:

[1]Department of Earth and Environmental Sciences, University of Rochester, Rochester, New York 14627; email: carmala.garzione@rochester.edu

[2]Department of Geology and Planetary Science, University of Pittsburgh, Pittsburgh, Pennsylvania 15260

[3]Institute for Geophysics and Department of Geological Sciences, Jackson School of Geosciences, University of Texas, Austin, Texas 78712

[4]Department of Geology and Geophysics, Texas A&M University, College Station, Texas 77843

[5]Department of Geosciences, University of Tübingen, Tübingen 72074, Germany

[6]Department of Geosciences, University of Arizona, Tucson, Arizona 85721

[7]Department of Earth and Planetary Sciences, Washington University, St. Louis, Missouri 63130

[8]StructureSolver LLC, Danville, California 94526

[9]Department of Geology, Macalester College, St. Paul, Minnesota 55105

[10]Faculty of Geology and Geophysics, University of Bucharest 010041, Romania

[11]The United States Geological Survey, Anchorage, Alaska 99508

[12]Department of Geological Sciences, University of Michigan, Ann Arbor, Michigan 48109

[13]Department of Terrestrial Magnetism, Carnegie Institution for Science, Washington, DC 20015

[14]Department of Earth and Atmospheric Sciences, University of Houston, Houston, Texas 77204

LITERATURE CITED

Allmendinger RW, Jordan TE, Kay SM, Isacks BL. 1997. The evolution of the Altiplano-Puna plateau of the Central Andes. *Annu. Rev. Earth Planet. Sci.* 25(1):139–74

Antonijevic SK, Wagner LS, Kumar A, Beck SL, Long MD, et al. 2015. The role of ridges in the formation and longevity of flat slabs. *Nature* 524(7564):212–15

Arriagada C, Roperch P, Mpodozis C, Dupont-Nivet G, Cobold PR, et al. 2003. Paleogene clockwise tectonic rotations in the fore-arc of central Andes, Antofagasta region, northern Chile. *J. Geophys. Res.* 108:2032

Arriagada C, Roperch P, Mpodozis C, Fernandez R. 2006. Paleomagnetism and tectonics of the southern Atacama Desert (25–28°S), northern Chile. *Tectonics* 25:TC4001

Baby P, Rochat P, Mascle G, Herail G. 1997. Neogene shortening contribution to crustal thickening in the back arc of the central Andes. *Geology* 25:883–86

Barke R, Lamb S. 2006. Late Cenozoic uplift of the Eastern Cordillera, Bolivian Andes. *Earth Planet. Sci. Lett.* 249(3):350–67

Barnes JB, Ehlers TA, Insel N, McQuarrie N, Poulsen CJ. 2012. Linking orography, climate, and exhumation across the central Andes. *Geology* 40:1135–38

Barnes JB, Ehlers TA, McQuarrie N, O'Sullivan PB, Pelletier JD. 2006. Eocene to recent variations in erosion across the central Andean fold-thrust belt, northern Bolivia: implications for plateau evolution: *Earth Planet. Sci. Lett.* 248:118–33

Barnes JB, Ehlers TA, McQuarrie N, O'Sullivan PB, Tawackoli PB. 2008. Thermochronometer record of central Andean Plateau growth, Bolivia (19.5°S). *Tectonics* 27:TC3003

Baumont D, Paul A, Zandt G, Beck SL, Pedersen B. 2002. Lithospheric structure of the central Andes based on surface wave dispersion. *J. Geophys. Res.* 107:2371

Beck SL, Zandt G. 2002. The nature of orogenic crust in the central Andes. *J. Geophy. Res. Solid Earth* 107:2230

Beck SL, Zandt G, Wagner L. 2010. Central Andean uplift and the geodynamics of the high topography. *International Federation of Digital Seismography Networks*. Other/Seismic Network. **https//doi.org/10.7914/SN/ZG_2010**

Benjamin MT, Johnson NM, Naeser CW. 1987. Recent rapid uplift in the Bolivian Andes: evidence from fission-track dating. *Geology* 15:680–83

Bershaw J, Garzione CN, Higgins P, MacFadden BJ, Anaya F, et al. 2010. Spatial-temporal changes in Andean plateau climate and elevation from stable isotopes of mammal teeth. *Earth Planet. Sci. Lett.* 289(3):530–38

Bird P. 1978. Finite element modeling of lithosphere deformation: the Zagros collision orogeny. *Tectonophysics* 50(2):307–36

Carlier G, Lorand JP, Liégeois JP, Fornari M, Soler P, et al. 2005. Potassic-ultrapotassic mafic rocks delineate two lithospheric mantle blocks beneath the southern Peruvian Altiplano. *Geology* 33:601–4

Carlotto V. 2013. Paleogeographic and tectonic controls on the evolution of Cenozoic basins in the Altiplano and Western Cordillera of southern Peru. *Tectonophysics* 589:195–219

Chapman AD, Ducea MN, McQuarrie N, Coble M, Petrescu L, et al. 2015. Constraints on plateau architecture and assembly from deep crustal xenoliths, Northern Altiplano (SE Peru). *Geol. Soc. Am. Bull.* 127(11–12):1777–97

Chiaradia M. 2015. Crustal thickness control on Sr/Y signatures of recent arc magmas: an Earth scale perspective. *Sci. Rep.* 5:8115

Chong G. 1977. Contributions to the knowledge of the Domeyko range in the Andes of northern Chile. *Geol. Rundsch.* 66:374–404

Cobbold PR, Rossello EA, Roperch P, Arriagada C, Gómez LA, Lima C. 2007. Distribution, timing, and causes of Andean deformation across South America. *Geol. Soc. Lond. Spec. Publ.* 272(1):321–43

Coney PJ, Evenchick CA. 1994. Consolidation of the American Cordilleras. *J. S. Am. Earth Sci.* 7:241–62

DeCelles PG, Ducea MN, Kapp P, Zandt G. 2009. Cyclicity in Cordilleran orogenic systems. *Nat. Geosci.* 2:251–57

DeCelles PG, Carrapa B, Horton BK, McNabb J, Gehrels GE, et al. 2015a. The Miocene Arizaro basin, central Andean hinterland: Response to partial lithosphere removal? See DeCelles et al. 2015b, pp. 359–86

DeCelles PG, Ducea MN, Carrapa B, Kapp AP, eds. 2015b. *Geodynamics of a Cordilleran Orogenic System: The Central Andes of Argentina and Northern Chile*, GSA Mem. 212. Boulder, CO: Geol. Soc. Am.

Demouy S, Paquette J-L, de Saint Blanquat M, Benoit M, Belousova EA, et al. 2012. Spatial and temporal evolution of Liassic to Paleocene arc activity in southern Peru unraveled by zircon U-Pb and Hf in-situ data on plutonic rocks. *Lithos* 155:183–200

Ducea MN, Seclaman AC, Murray KE, Jianu D, Schoenbohm LM. 2013. Mantle-drip magmatism beneath the Altiplano-Puna plateau, central Andes. *Geology* 41:915–18

Ducea MN, Paterson SR, DeCelles PG. 2015a. High-volume magmatic events in subduction systems. *Elements* 11(2):99–104

Ducea MN, Saleeby JB, Bergantz G. 2015b. The architecture, chemistry, and evolution of continental magmatic arcs. *Annu. Rev. Earth Planet. Sci.* 43:299–331

Echavarria L, Hernández R, Allmendinger R, Reynolds J. 2003. Subandean thrust and fold belt of northwestern Argentina: geometry and timing of the Andean evolution. *AAPG Bull*. 87:965–85

Eichelberger N, McQuarrie N, Ehlers TA, Enkelmann E, Barnes JB, Lease RO. 2013. New constraints on the chronology, magnitude, and distribution of deformation within the central Andean orocline. *Tectonics* 32:1432–53

Eichelberger N, McQuarrie N, Ryan J, Karimi B, Beck S, Zandt G. 2015. Evolution of crustal thickening in the central Andes, Bolivia. *Earth Planet. Sci. Lett.* 426:191–203

Ehlers TA. 2005. Crustal thermal processes and thermochronometer interpretation. *Rev. Mineral. Geochem.* 58:315–50

Ehlers TA, Poulsen CJ. 2009. Influence of Andean uplift on climate and paleoaltimetry estimates. *Earth Planet. Sci. Lett.* 281(3):238–48

Farrar E, Clark AH, Kontak DJ, Archibald DA. 1988. Zongo-San Gabon zone: Eocene foreland boundary of Central Andean orogen, northwest Bolivia and southeast Peru. *Geology* 16:55–58

Feng R, Poulsen CJ. 2016. Refinement of Eocene lapse rates, fossil-leaf altimetry, and North American Cordilleran surface elevation estimates. *Earth Planet. Sci. Lett.* 436:130–41

Feng R, Poulsen CJ, Werner M, Chamberlain CP, Mix HT, et al. 2013. Early Cenozoic evolution of topography, climate, and stable isotopes in precipitation in the North American Cordillera. *Am. J. Sci.* 313(7):613–48

Fiorella RP, Poulsen CJ, Zolá RS, Jeffery ML, Ehlers TA. 2015. Modern and long-term evaporation of central Andes surface waters suggests paleo archives underestimate Neogene elevations. *Earth Planet. Sci. Lett.* 432:59–72

Fox M, Bodin T, Shuster DL. 2015. Abrupt changes in the rate of Andean Plateau uplift from reversible jump Markov Chain Monte Carlo inversion of river profiles. *Geomorphology* 238:1–14

Garzione CN, Auerbach D, Smith JJ, Rosario J, Passey BH, et al. 2014. Clumped isotope evidence for diachronous surface cooling of the Altiplano and pulsed surface uplift of the Central Andes. *Earth Planet. Sci. Lett.* 393:173–81

Garzione CN, Hoke GD, Libarkin JC, Withers S, MacFadden BJ, et al. 2008. Rise of the Andes. *Science* 320:1304–7

Garzione CN, Molnar P, Libarkin JC, MacFadden BJ. 2006. Rapid late Miocene rise of the Bolivian Altiplano: evidence for removal of mantle lithosphere. *Earth Planet. Sci. Lett.* 241:543–56

Ghosh P, Garzione CN, Eiler JM. 2006. Rapid uplift of the Altiplano revealed through 13C-18O bonds in paleosol carbonates. *Science* 311(5760):511–15

Gillis RJ, Horton BK, Grove M. 2006. Thermochronology, geochronology, and upper crustal structure of the Cordillera Real: implications for Cenozoic exhumation of the central Andean plateau. *Tectonics* 25:TC6007

Gotberg N, McQuarrie N, Caillaux VC. 2010. Comparison of crustal thickening budget and shortening estimates in southern Peru (12–14°S): implications for mass balance and rotations in the "Bolivian orocline." *Geol. Soc. Am. Bull.* 122:727–42

Graham A, Gregory-Wodzicki KM, Wright KL. 2001. Studies in Neotropical Paleobotany. XV. A Mio-Pliocene palynoflora from the Eastern Cordillera, Bolivia: implications for the uplift history of the Central Andes. *Am. J. Bot.* 88(9):1545–57

Gregory-Wodzicki KM. 2000. Uplift history of the Central and Northern Andes: a review. *Geol. Soc. Am. Bull.* 112(7):1091–105

Gregory-Wodzicki KM. 2002. A late Miocene subtropical-dry flora from the northern Altiplano, Bolivia. *Palaeogeogr. Palaeoclimatol. Palaeoecol.* 180(4):331–48

Gregory-Wodzicki KM, McIntosh WC, Velasquez K. 1998. Climatic and tectonic implications of the late Miocene Jakokkota flora, Bolivian Altiplano. *J. S. Am. Earth Sci.* 11(6):533–60

Gubbels TL, Isacks BL, Farrar E. 1993. High-level surfaces, plateau uplift, and foreland development, Bolivian central Andes. *Geology* 21:695–98

Haschke M, Guenther A. 2003. Balancing crustal thickening in arcs by tectonic vs. magmatic means. *Geology* 31:933–36

Hayes GP, Wald DJ, Johnson RL. 2012. Slab1.0: A three-dimensional model of global subduction zone geometries. *J. Geophys. Res.* 117:B01302

Heit B, Sodoudi F, Yuan X, Bianchi M, Kind R. 2007. An S receiver function analysis of the lithospheric structure in South America. *Geophy. Res. Lett.* 34:L14307

Hoke GD, Garzione CN. 2008. Paleosurfaces, paleoelevation, and the mechanisms for the late Miocene topographic development of the Altiplano plateau. *Earth Planet. Sci. Lett.* 271(1):192–201

Hoke GD, Isacks BL, Jordan TE, Blanco N, Tomlinson AJ, et al. 2007. Geomorphic evidence for post-10 Ma uplift of the western flank of the central Andes 18°30′–22°S. *Tectonics* 26(5):TC5021

Horton BK. 1999. Erosional control on the geometry and kinematics of thrust belt development in the central Andes. *Tectonics* 18:1292–304

Horton BK. 2012. Cenozoic evolution of hinterland basins in the Andes and Tibet. In *Tectonics of Sedimentary Basins: Recent Advances*, ed. C Busby, A Azor, pp. 427–44. Oxford, UK: Wiley-Blackwell

Horton BK, Hampton BA, LaReau BN, Baldellón E. 2002. Tertiary provenance history of the northern and central Altiplano (central Andes, Bolivia): a detrital record of plateau-margin tectonics. *J. Sediment. Res.* 72:711–26

Horton BK, Hampton BA, Waanders GL. 2001. Paleogene synorogenic sedimentation in the Altiplano plateau and implications for initial mountain building in the central Andes. *Geol. Soc. Am. Bull.* 113:1387–400

Horton BK, Perez ND, Fitch JD, Saylor JE. 2015. Punctuated shortening and subsidence in the Altiplano Plateau of southern Peru: implications for early Andean mountain building. *Lithosphere* 7(2):117–37

Houseman GA, McKenzie D, Molnar P. 1981. Convective instability of a thickened boundary layer and its relevance for the thermal evolution of continental convergent belts. *J. Geophys. Res.* 86 (B7):6115–32

Husson L, Sempere T. 2003. Thickening the Altiplano crust by gravity-driven crustal channel flow. *Geophys. Res. Lett.* 30(5):1243

Insel N, Poulsen CJ, Ehlers TA. 2010. Influence of the Andes Mountains on South American moisture transport, convection, and precipitation. *Climate Dyn.* 35 (7–8):1477–92

Insel N, Poulsen CJ, Ehlers TA, Sturm C. 2012. Response of meteoric $\delta^{18}O$ to surface uplift—implications for Cenozoic Andean Plateau growth. *Earth Planet. Sci. Lett.* 317:262–72

Isacks BL. 1988. Uplift of the Central Andean Plateau and bending of the Bolivian orocline. *J. Geophys. Res.* 93:3211–31

James DE, Sacks S. 1999. Cenozoic formation of the central Andes: a geophysical perspective. In *Geology and Ore Deposits of the Central Andes*, Vol. 7, ed. BJ Skinner, pp. 1–25. Littleton, CO: Soc. Econ. Geol.

Jeffery ML, Poulsen CJ, Ehlers TA. 2012. Impacts of Cenozoic global cooling, surface uplift, and an inland seaway on South American paleoclimate and precipitation $\delta^{18}O$. *Geol. Soc. Am. Bull.* 124(3–4):335–51

Jeffery ML, Ehlers TA, Yanites BJ, Poulsen CJ. 2013. Quantifying the role of paleoclimate and Andean Plateau uplift on river incision. *J. Geophys. Res. Earth Surf.* 118(2):852–71

Jordan T, Nester P, Blanco N, Hoke G, Davila F, Tomlinson A. 2010. Uplift of the Altiplano-Puna plateau: a view from the west. *Tectonics* 29:TC5007

Kar N, Garzione CN, Jaramillo C, Shanahan T, Carlotto V, et al. 2016. Rapid regional surface uplift of the northern Altiplano plateau revealed by multiproxy paleoclimate reconstruction. *Earth Planet. Sci. Lett.* 447:33–47

Kay RF, MacFadden BJ, Madden RH, Sandeman H, Anaya F. 1998. Revised age of the Salla beds, Bolivia, and its bearing on the age of the Deseadan South American Land Mammal "Age." *J. Vertebr. Paleontol.* 18:189–99

Kay SM, Coira BL. 2009. Shallowing and steepening subduction zones, continental lithospheric loss, magmatism, and crustal flow under the Central Andean Altiplano-Puna Plateau. In *Backbone of the Americas: Shallow Subduction, Plateau Uplift, and Ridge and Terrane Collision*, ed. SM Kay, VA Ramos, WR Dickinson, pp. 229–59. Boulder, CO: Geol. Soc. Am.

Kennan L, Lamb SH, Hoke L. 1997. High-altitude palaeosurfaces in the Bolivian Andes: evidence for late Cenozoic surface uplift. *Geol. Soc. Lond. Spec. Publ.* 120(1):307–23

Kley J. 1996. Transition from basement-involved to thin-skinned thrusting in the Cordillera Oriental of southern Bolivia. *Tectonics* 15:763–75

Kontak DJ, Farrar E, Clark A, Archibald DA. 1990. Eocene tectono-thermal rejuvenation of an Upper Paleozoic-Lower Mesozoic terrane in the Cordillera de Carabaya, Puno, southeastern Peru, revealed by K–Ar and ^{40}Ar/^{39}Ar dating. *J. S. Am. Earth Sci.* 3:231–46

Kumar A, Wagner LS, Beck SL, Long MD, Zandt G, et al. 2016. Seismicity and state of stress in the central and southern Peruvian flat slab. *Earth Planet. Sci. Lett.* 441:71–80

Krystopowicz NJ, Currie CA. 2013. Crustal eclogitization and lithosphere delamination in orogens. *Earth Planet. Sci. Lett.* 361:195–207

Lamb S. 2011. Did shortening in thick crust cause rapid late Cenozoic uplift in the northern Bolivian Andes? *J. Geol. Soc.* 168:1079–92

Lamb S, Hoke L. 1997. Origin of the high plateau in the Central Andes, Bolivia, South America. *Tectonics* 16:623–49

Lease RO, Ehlers TA. 2013. Incision into the eastern Andean plateau during Pliocene cooling. *Science* 341(6147):774–76

Lease RO, Ehlers TA, Enkelmann E. 2016. Large along-strike variations in the onset of Subandean exhumation: implications for Central Andean orogenic growth. *Earth Planet. Sci. Lett.* 451:62–76

Leier AL, McQuarrie N, Horton BK, Gehrels GE. 2010. Upper Oligocene conglomerates of the Altiplano, Central Andes: the record of deposition and deformation along the margin of a hinterland basin. *J. Sediment. Res.* 80:750–62

Leier A, McQuarrie N, Garzione CN, Eiler JM. 2013. Stable isotope evidence for multiple pulses of rapid surface uplift in the Central Andes, Bolivia. *Earth Planet. Sci. Lett.* 371:49–58

Long MD, Biryol CB, Eakin CM, Beck SL, Wagner LS, et al. 2016. Overriding plate, mantle wedge, slab, and subslab contributions to seismic anisotropy beneath the northern Central Andean Plateau. *Geochem. Geophys. Geosyst.* 17:2556–75

Ma Y, Clayton RW. 2014. The crust and uppermost mantle structure of Southern Peru from ambient noise and earthquake surface wave analysis. *Earth Planet. Sci. Lett.* 395:61–70

Maksaev Y, Boric R, Zentilli M, Reynolds PH. 1988. Metallogenetic implications of K–Ar, [40]Ar–[39]Ar, and fission track dates of mineralized areas in the Andes of northern Chile. *V. Congr. Geol. J. Chil. Aetas* 1:B65–86

Mamani M, Worner G, Sempere T. 2010. Geochemical variations in igneous rocks of the Central Andean orocline (13°S to 18°S): tracing crustal thickening and magma generation through time. *Geol. Soc. Am. Bull.* 122:162–82

McLeod CL, Davidson JP, Nowell GM, de Silva SL, Schmitt AK. 2013. Characterizing the continental basement of the Central Andes: constraints from Bolivian crustal xenoliths. *Geol. Soc. Am. Bull.* 125:985–97

McBride SL, Clark AH, Farrar E, Archibald DA. 1987. Delimitation of a cryptic Eocene tectono-thermal domain in the Eastern Cordillera of the Bolivian Andes through K–Ar dating and [40]Ar–[39]Ar step-heating. *J. Geol. Soc.* 144:243–55

McQuarrie N. 2002. The kinematic history of the central Andean fold-thrust belt, Bolivia: implications for building a high plateau: *Geol. Soc. Am. Bull.* 114:950–63

McQuarrie N, DeCelles P. 2001. Geometry and structural evolution of the central Andean backthrust belt, Bolivia. *Tectonics* 20(5):669–92

McQuarrie N, Horton BK, Zandt G, Beck S, DeCelles PG. 2005. Lithospheric evolution of the Andean fold-thrust belt, Bolivia, and the origin of the central Andean plateau. *Tectonophysics* 399:15–37

McQuarrie N, Barnes JB, Ehlers TA. 2008. Geometric, kinematic, and erosional history of the central Andean Plateau, Bolivia (15–17°S). *Tectonics* 27:TC3007

McQuarrie N, Ehlers TA. 2015. Influence of thrust belt geometry and shortening rate on thermochronometer cooling ages: insights from the Bhutan Himalaya. *Tectonics* 34:1055–79

McQuarrie N, Ehlers TA. 2017. Techniques for understanding fold-thrust belt kinematics and thermal evolution. In *Linkages and Feedbacks in Orogenic Processes*, GSA Mem. 213, ed. RD Law, JR Thigpen, AJ Merschat, HH Stowell, pp. 1–30. Boulder, CO: Geol. Soc. Am. In press

McQuarrie N, Rak AJ, Ehlers T. 2015. *Constraining age and rate of deformation in the northern Bolivian Andes from cross sections, cooling ages, and thermokinematic modeling.* Presented at Fall Meet., AGU, San Francisco (Abstr. T34A-03)

Mégard F. 1978. Étude géologique des Andes du Pérou central. Mem. 86. Paris: ORSTOM

Mégard F. 1984. The Andean orogenic period and its major structures in central and northern Peru. *J. Geol. Soc. Lond.* 141:893–900

Mégard F. 1987. Cordilleran Andes and marginal Andes: a review of Andean geology north of the Arica elbow (18°S). In *Circum-Pacific Orogenic Belts and Evolution of the Pacific Ocean Basin*, ed. JWH Monger, J Francheteau, *Geodyn. Monogr.* 18:71–95. Washington, DC: AGU

Mosolf JG, Horton BK, Heizler MT, Matos R. 2011. Unroofing the core of the central Andean fold-thrust belt during focused late Miocene exhumation: evidence from the Tipuani-Mapiri wedge-top basin, Bolivia. *Basin Res.* 23(3):346–60

Mpodozis C, Arriagada C, Basso M, Roperch P, Cobbold P, et al. 2005. Late Mesozoic to Paleogene stratigraphy of the Salar de Atacama basin, Antofagasta, Northern Chile: implications for the tectonic evolution of the central Andes. *Tectonophysics* 399:125–54

Mulch A, Uba CE, Strecker MR, Schoenberg R, Chamberlain CP. 2010. Late Miocene climate variability and surface elevation in the central Andes. *Earth Planet. Sci. Lett.* 290(1):173–82

Müller JP, Kley J, Jacobshagen V. 2002. Structure and Cenozoic kinematics of the Eastern Cordillera, southern Bolivia (21°S). *Tectonics* 21:1037

Murray BP, Horton BK, Matos R, Heizler MT. 2010. Oligocene–Miocene basin evolution in the northern Altiplano, Bolivia: implications for evolution of the central Andean backthrust belt and high plateau. *Geol. Soc. Am. Bull.* 122:1443–62

Myers S, Beck S, Zandt G, Wallace T. 1998. Lithospheric-scale structure across the Bolivian Andes from tomographic images of velocity and attenuation for *P* and *S* waves. *J. Geophys. Res*. 103:21233–52

Oncken O, Hindle D, Kley J, Elger K, Victor P, et al. 2006. Deformation of the central Andean upper plate system—facts, fiction, and constraints for plateau models. In *The Andes: Active Subduction Orogeny—Frontiers in Earth Sciences*, ed. O Oncken, G Chong, G Franz, P Giese, H-J Götze, et al., pp. 3–27. New York/Berlin: Springer-Verlag

Perkins JP, Finnegan NJ, Henderson ST, Rittenour TM. 2016. Topographic constraints on magma accumulation below the actively uplifting Uturuncu and Lazufre volcanic centers in the Central Andes. *Geosphere* 12(4):1078–96

Perez ND, Horton BK. 2014. Oligocene-Miocene deformational and depositional history of the Andean hinterland basin in the northern Altiplano plateau southern Peru. *Tectonics* 33:1819–47

Perez ND, Horton BK, Carlotto V. 2016a. Structural inheritance and selective reactivation in the central Andes: Cenozoic deformation guided by pre-Andean structures in southern Peru. *Tectonophysics* 671:264–80

Perez ND, Horton BK, McQuarrie N, Stubner K, Ehlers TA. 2016b. Andean shortening, inversion and exhumation associated with thin- and thick-skinned deformation in southern Peru. *Geol. Mag.* 153:1013–41

Phillips K, Clayton R, Davis P, Tavera H, Guy R, et al. 2012. Structure of the subduction system in southern Peru from seismic array data. *J. Geophy. Res.* 117:B11306

Picard D, Sempere T, Plantard O. 2008. Direction and timing of uplift propagation in the Peruvian Andes deduced from the molecular phylogeny of highland biotaxa. *Earth Planet. Sci. Lett.* 271:326–36

Pope DC, Willett SD. 1998. Thermal-mechanical model for crustal thickening in the central Andes driven by ablative subduction. *Geology* 26(6):511–14

Poulsen CJ, Ehlers TA, Insel N. 2010. Onset of convective rainfall during gradual late Miocene rise of the central Andes. *Science* 328(5977):490–93

Poulsen CJ, Jeffery ML. 2011. Climate change imprinting on stable isotopic compositions of high-elevation meteoric water cloaks past surface elevations of major orogens. *Geology* 39(6):595–98

Profeta L, Ducea MN, Chapman JB, Paterson SR, Henriquez Gonzales SM, et al. 2015. Quantifying crustal thickness over time in magmatic arcs. *Sci. Rep.* 5:17786

Rak AJ. 2015. *Geometry, kinematics, exhumation and sedimentation of the northern Bolivian fold-thrust-belt foreland basin system*. MS thesis, Univ. Pittsburgh, 121 pp.

Ryan J, Beck S, Zandt G, Wagner L, Minaya E, Taverna H. 2016. Central Andean crustal structure from receiver function analysis. *Tectonophysics* 682:120–33

Rech JA, Currie BS, Michalski G, Cowan AM. 2006. Neogene climate change and uplift in the Atacama Desert, Chile. *Geology* 34(9):761–64

Roperch P, Sempere T, Macedo O, Arriagada C, Fornari M, et al. 2006. Counterclockwise rotation of late Eocene–Oligocene fore-arc deposits in southern Peru and its significance for oroclinal bending in the central Andes. *Tectonics* 25:TC3010

Safran EB, Blythe AE, Dunne T. 2006. Spatially variable exhumation rates in orogenic belts: an Andean example. *J. Geol.* 114:665–81

Sandeman HA, Clark AH, Farrar E. 1995. An integrated tectono-magmatic model for the evolution of the southern Peruvian Andes (13–20°S) since 55 Ma. *Int. Geol. Rev.* 37:1039–73

Saylor JE, Horton BK. 2014. Nonuniform surface uplift of the Andean plateau revealed by deuterium isotopes in Miocene volcanic glass from southern Peru. *Earth Planet. Sci. Lett.* 387:120–31

Schildgen TF, Hodges KV, Whipple KX, Reiners PW, Pringle MS. 2007. Uplift of the western margin of the Andean plateau revealed from canyon incision history, southern Peru. *Geology* 35:523–26

Schildgen TF, Hodges KV, Whipple KX, Pringle MS, van Soest M, et al. 2009a. Late Cenozoic structural and tectonic development of the western margin of the central Andean Plateau in southwest Peru. *Tectonics* 28(4):TC4007

Schildgen TF, Ehlers TA, Whipp DM Jr., van Soest MC, Whipple KXl. 2009b. Quantifying canyon incision and Andean Plateau surface uplift, southwest Peru: a thermochronometer and numerical modeling approach. *J. Geophy. Res.* 114(F4):F04014

Scheuber E, Reutter KJ. 1992. Magmatic arc tectonics in the Central Andes between 21° and 25°S. *Tectonophysics* 205:127–40

Scheuber E, Mertmann D, Ege H, Silva-Gonzalez P, Heubeck C, et al. 2006. Exhumation and basin development related to formation of the Central Andean Plateau, 21°S. In *The Andes: Active Subduction Orogeny—Frontiers in Earth Sciences*, ed. O Oncken, G Chong, G Franz, P Giese, H-J Götze, et al., pp. 285–301. New York/Berlin: Springer-Verlag

Sempere T, Hérail G, Oller J, Bonhomme MG. 1990. Late Oligocene–Early Miocene major tectonic crisis and related basins in Bolivia. *Geology* 18(10):946–49

Sobolev SV, Babeyko AY. 2005. What drives orogeny in the Andes? *Geology* 33(8):617–20

Swenson J, Beck S, Zandt G. 1999. Regional distance shear-coupled PL propagation within the northern Altiplano, central Andes. *Geophys. J. Int.* 139:743–53

Tassara A, Echaurren A. 2012. Anatomy of the Andean subduction zone: three-dimensional density model upgraded and compared against global-scale models. *Geophy. J. Int.* 189(1):161–68

Thouret JC, Worner G, Gunnell Y, Singer B, Zhang X, et al. 2007. Geochronologic and stratigraphic constraints on canyon incision and Miocene uplift of the Central Andes in Peru. *Earth Planet. Sci. Lett.* 263:151–66

Tao WC, O'Connell RJ. 1992. Ablative subduction: a two-sided alternative to the conventional subduction model. *J. Geophy. Res.* 97(B6):8877–904

Turner SJ, Langmuir CH. 2015. The global chemical systematics of arc front stratovolcanoes: evaluating the role of crustal processes. *Earth Planet. Sci. Lett.* 422:182–93

Uba CE, Kley J, Strecker MR, Schmitt A. 2009. Unsteady evolution of the Bolivian Subandean thrust belt: the role of enhanced erosion and clastic wedge progradation. *Earth Planet. Sci. Lett.* 281:134–46

Wagner L, Beck S, Long M. 2010. PerU Lithosphere and Slab Experiment. *International Federation of Digital Seismography Networks*. Other/Seismic Network. **http://www.fdsn.org/networks/detail/ZD_2010**

Wagner LS, Beck S, Zandt G. 2005. Upper mantle structure in the south central Chilean subduction zone (30° to 36°S). *J. Geophys. Res.* 110(B1):B01308

Wagner LS, Beck S, Zandt G, Ducea MN. 2006. Depleted lithosphere, cold, trapped asthenosphere, and frozen melt puddles above the flat slab in central Chile and Argentina. *Earth Planet. Sci. Lett.* 245:289–301

Wang H, Currie CA, DeCelles PG. 2015. Hinterland basin formation and gravitational instabilities in the central Andes: constraints from gravity data and geodynamic models. See DeCelles et al. 2015b, pp. 387–406

Ward KM, Porter RC, Zandt G, Beck SL, Wagner LS, et al. 2013. Ambient noise tomography across the Central Andes. *Geophy. J. Int.* 194:1559–73

Ward KM, Zandt G, Beck SL, Wagner LS, Taverna H. 2016. Lithospheric structure beneath the northern Central Andean Plateau from the joint inversion of ambient noise and earthquake-generated surface waves. *J. Geophy. Res.* 121:8217–38

Whipple KX, Gasparini NM. 2014. Tectonic control of topography, rainfall patterns, and erosion during rapid post–12 Ma uplift of the Bolivian Andes. *Lithosphere* 6(4):251–68

Contents

Errata

An online log of corrections to *Annual Review of Earth and Planetary Sciences* articles
may be found at http://www.annualreviews.org/errata/earth